Article

Current Biology

Pedomorphosis in the ancestry of marsupial mammals

Highlights

- Cranial shape develops in a cone-shaped pattern with a conserved fetal region
- Placental altricial-precocial developmental strategy impacts cranial morphology
- A novel hypothesis for the evolution of mammal skull development is proposed
- Marsupials reflect a more derived state of mammal skull development than placentals

Authors

Heather E. White, Abigail S. Tucker, Vincent Fernandez, ..., Daniel J. Urban, Karen E. Sears, Anjali Goswami

Correspondence

h.white@nhm.ac.uk

In brief

White et al. quantify cranial ontogenetic trajectories and estimate ancestral states to reassess biases in interpreting the evolution of mammal development. Pedomorphosis occurs on the marsupial lineage, diverging from ancestral placental and ancestral therian trajectories. Marsupials reflect the most derived state of mammal cranial development.

White et al., 2023, Current Biology *33*, 1–15
June 5, 2023
https://doi.org/10.1016/j.cub.2023.04.009

CellPress

Current Biology

CellPress
OPEN ACCESS

Article

Pedomorphosis in the ancestry of marsupial mammals

Heather E. White,[1,2,3,9,11,*] Abigail S. Tucker,[2] Vincent Fernandez,[4] Roberto Portela Miguez,[1] Lionel Hautier,[1,5] Anthony Herrel,[6] Daniel J. Urban,[7] Karen E. Sears,[8] and Anjali Goswami[1,3,10]

[1]Science Department, Natural History Museum, Cromwell Road, London SW7 5BD, UK
[2]Centre for Craniofacial and Regenerative Biology, King's College London, Great Maze Pond, London SE1 9RT, UK
[3]Division of Biosciences, University College London, Gower Street, London WC1E 6DE, UK
[4]European Synchrotron Radiation Facility, 71 rue des Martyrs, 38000 Grenoble, France
[5]Institut des Sciences de l'Evolution, Université de Montpellier, CNRS, IRD, EPHE, Montpellier 34095, France
[6]UMR 7179, Centre National de la Recherche Scientifique/Muséum National d'Histoire Naturelle, Département Adaptations du Vivant, 55 rue Buffon, 75005 Paris, France
[7]Institute of Genomic Biology, University of Illinois, Urbana, IL 61801, USA
[8]Department of Ecology and Evolutionary Biology, University of California Los Angeles, Los Angeles, CA 90095, USA
[9]Twitter: @heather_e_white
[10]Twitter: @anjgoswami
[11]Lead contact
*Correspondence: h.white@nhm.ac.uk
https://doi.org/10.1016/j.cub.2023.04.009

SUMMARY

Within mammals, different reproductive strategies (e.g., egg laying, live birth of extremely underdeveloped young, and live birth of well-developed young) have been linked to divergent evolutionary histories. How and when developmental variation across mammals arose is unclear. While egg laying is unquestionably considered the ancestral state for all mammals, many long-standing biases treat the extreme underdeveloped state of marsupial young as the ancestral state for therian mammals (clade including both marsupials and placentals), with the well-developed young of placentals often considered the derived mode of development. Here, we quantify mammalian cranial morphological development and estimate ancestral patterns of cranial shape development using geometric morphometric analysis of the largest comparative ontogenetic dataset of mammals to date (165 specimens, 22 species). We identify a conserved region of cranial morphospace for fetal specimens, after which cranial morphology diversified through ontogeny in a cone-shaped pattern. This cone-shaped pattern of development distinctively reflected the upper half of the developmental hourglass model. Moreover, cranial morphological variation was found to be significantly associated with the level of development (position on the altricial-precocial spectrum) exhibited at birth. Estimation of ancestral state allometry (size-related shape change) reconstructs marsupials as pedomorphic relative to the ancestral therian mammal. In contrast, the estimated allometries for the ancestral placental and ancestral therian were indistinguishable. Thus, from our results, we hypothesize that placental mammal cranial development most closely reflects that of the ancestral therian mammal, while marsupial cranial development represents a more derived mode of mammalian development, in stark contrast to many interpretations of mammalian evolution.

INTRODUCTION

All living mammals shared a common ancestor that lived at least 165 million years ago.[1,2] The mammalian crown group is defined by the divergence of monotremes from therians, which themselves diverged into the modern lineages of marsupials and placentals approximately 160 million years ago.[3,4] These three extant mammal infraclasses are easily recognized by their diverse and distinct modes of reproduction. Monotremes are oviparous (egg laying), while therians are viviparous (giving birth to live young). However, within therians, marsupials have a highly restricted gestation period (around 12–38 days) after which they give birth to tiny poorly developed young (approximately 5 mg to 0.5 g)[5] in a highly altricial state with limited skeletal morphogenesis and organogenesis.[6] In contrast, placentals give birth to more developed young following lengthier gestation, ranging from a minimum of 13–20 days in some shrews to approximately 660 days in *Loxodonta africana* (African elephant), with birth weights spanning from 0.2 g (*Suncus etruscus*) to 91 kg (*Loxodonta africana*)[5,7,8] (note we use the term placental here to refer to crown eutherian mammals, but we recognize that marsupials also have placenta). Species from the four major placental superorders span a wide range of the altricial-precocial spectrum,[9,10] although none are as highly altricial as marsupials.[11–13] Many studies and long-standing biases view the marsupial mode of development as an evolutionary stepping stone between monotremes and placentals,[14,15] and they consequently consider the marsupial mode to be more primitive than the

Please cite this article in press as: White et al., Pedomorphosis in the ancestry of marsupial mammals, Current Biology (2023), https://doi.org/10.1016/j.cub.2023.04.009

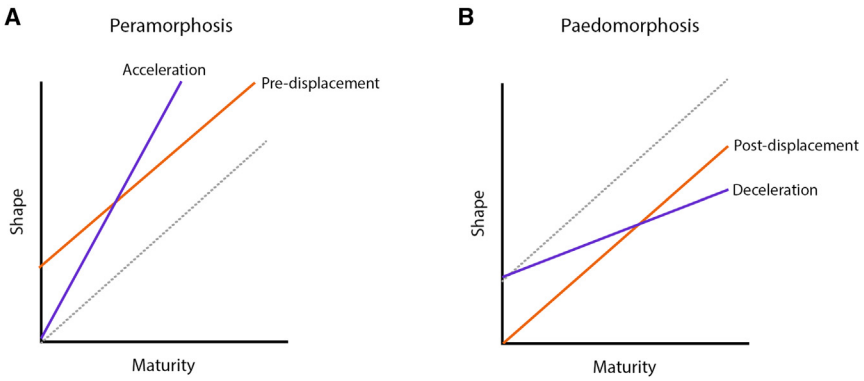

Figure 1. Theoretical ontogenetic trajectories depicting heterochronic shifts

The dashed gray line represents the theoretical ancestral trajectory, while the solid purple line represents changes in developmental rate, and the solid red line represents differences in timing of onset of growth. Solid lines are compared with the dashed ancestral line to identify heterochronic shifts. This figure is based on descriptions from McNamara[30] and Morris et al.[32]

(A) Examples of peramorphosis.

(B) Examples of pedomorphosis.

placental mode.[6,15–18] This bias is further reflected in their total clade names: Prototheria (first beast), Metatheria (middle beast), and Eutheria (true beast).[19] Even though this bias of marsupial evolution is held by many, a few studies have argued otherwise, suggesting that marsupial development is instead highly derived.[20,21] The view of marsupials as "primitive" relative to placentals has been compounded by differences in their diversity. Specifically, the higher phenotypic and taxonomic diversity of placentals, as compared with marsupials, is often ascribed to the more derived placental developmental strategy.[17,18,22–24] Despite a long interest in the developmental differences among mammalian clades and their evolutionary significance, as well as increasing information from the fossil record,[25,26] the origins of the developmental diversity observed across Mammalia remains poorly understood.

Heterochrony (changes in timing, rate, or duration of developmental processes) is well established as a primary mechanism facilitating phenotypic evolution.[27–30] Heterochronic shifts result from either pedomorphosis (progenesis, post-displacement, and neoteny), where morphological development is slowed and the adult retains juvenile characteristics, or peramorphosis (hypermorphosis, pre-displacement, and acceleration) where maturation is delayed by extended growth periods[27,31] (Figure 1). Heterochrony can be studied by qualitative or quantitative comparison of sequences of developmental events, such as the relative timing and pattern of bone ossification.[33,34] Alternatively, geometric morphometric approaches, which have long been used to quantify and compare shape change through ontogeny,[27,35–39] can be used for identification of heterochronic shifts.[29,32,40–43]

Identifying when phenotypic diversity arises during development is critical for understanding how developmental processes shape phenotypic evolution. This particular topic has been long discussed in the context of the marsupial-placental dichotomy, due to their highly divergent developmental timings and patterns.[6,17,22,33,44–47] Marsupials are born in a highly altricial state, usually within a few weeks of conception. Immediately upon birth, neonates experience the intense functional demands of crawling to the teat and suckling intensively.[48] These functional requirements at such an early stage of development are thought to have driven heterochronic shifts in bone ossification,[28,33,44,47] with only the oral apparatus (for suckling) and forelimbs (for crawling to the teat) being well developed at birth.[17,22,28,33,34,44,48,49] This early ossification and functional load in turn is thought to have constrained the evolution of the marsupial skull, specifically the oral apparatus,[44,46,47,50,51] as well as the jaw,[52] forelimb,[18,23] and shoulder girdle,[22] reflected by reduced morphological disparity of these structures in marsupials relative to placentals.[22,46,53] This hypothesis has recently been challenged,[54–57] with the suggestion that developmental constraint on marsupial forelimbs are overridden by functional selection on a macroevolutionary timescale, particularly in specific ecological niches.[57] Nonetheless, most analyses support the hypothesis that developmental constraints limit the evolution of morphological variation in marsupials. Beyond this marsupial-placental dichotomy, placentals show extensive variation in altriciality and precociality[9,10,58]; however, the impact of these diverse strategies within placentals has received less attention than the marsupial-placental dichotomy.

Despite the well-appreciated importance of ontogeny in shaping the adult phenotype, there are relatively few studies that quantify shape, using geometric morphometrics, through ontogeny beyond those using model organisms (e.g., mouse). Of those that do, the vast majority focuses on the cranium, owing to both its developmental complexity and functional importance. Thus, the skull is one of the best studied skeletal elements within Mammalia[59–64] and therefore ideal for assessing macroevolutionary and developmental patterns. However, many studies analyzing cranial morphological development are limited to an individual species or single clade,[38,40,65–71] due to poor availability of ontogenetic specimens. Broader scale comparisons of ontogenetic trajectories are nevertheless required to deduce the influence of development or heterochronic shifts on macroevolutionary patterns.

Here, we address the question: how does variation in the development of skull shape influence mammalian cranial evolution? To do so, we apply a 3D geometric morphometric approach, using 69 landmarks, to quantify skull morphology through ontogeny with the largest dataset assembled to date, spanning the full phylogenetic breadth of mammals and ranging from fetal to adult specimens (22 species and 165 specimens) (Figure 2). Full details of the dataset, morphometric data collection, and analyses can be found in the STAR Methods section. Across this developmentally and ecologically diverse dataset of 22 extant mammalian taxa, we quantify the ontogeny of cranial morphological variation and estimate ancestral patterns of cranial shape development. With these results, we reconstruct the

Please cite this article in press as: White et al., Pedomorphosis in the ancestry of marsupial mammals, Current Biology (2023), https://doi.org/10.1016/j.cub.2023.04.009

CellPress
OPEN ACCESS

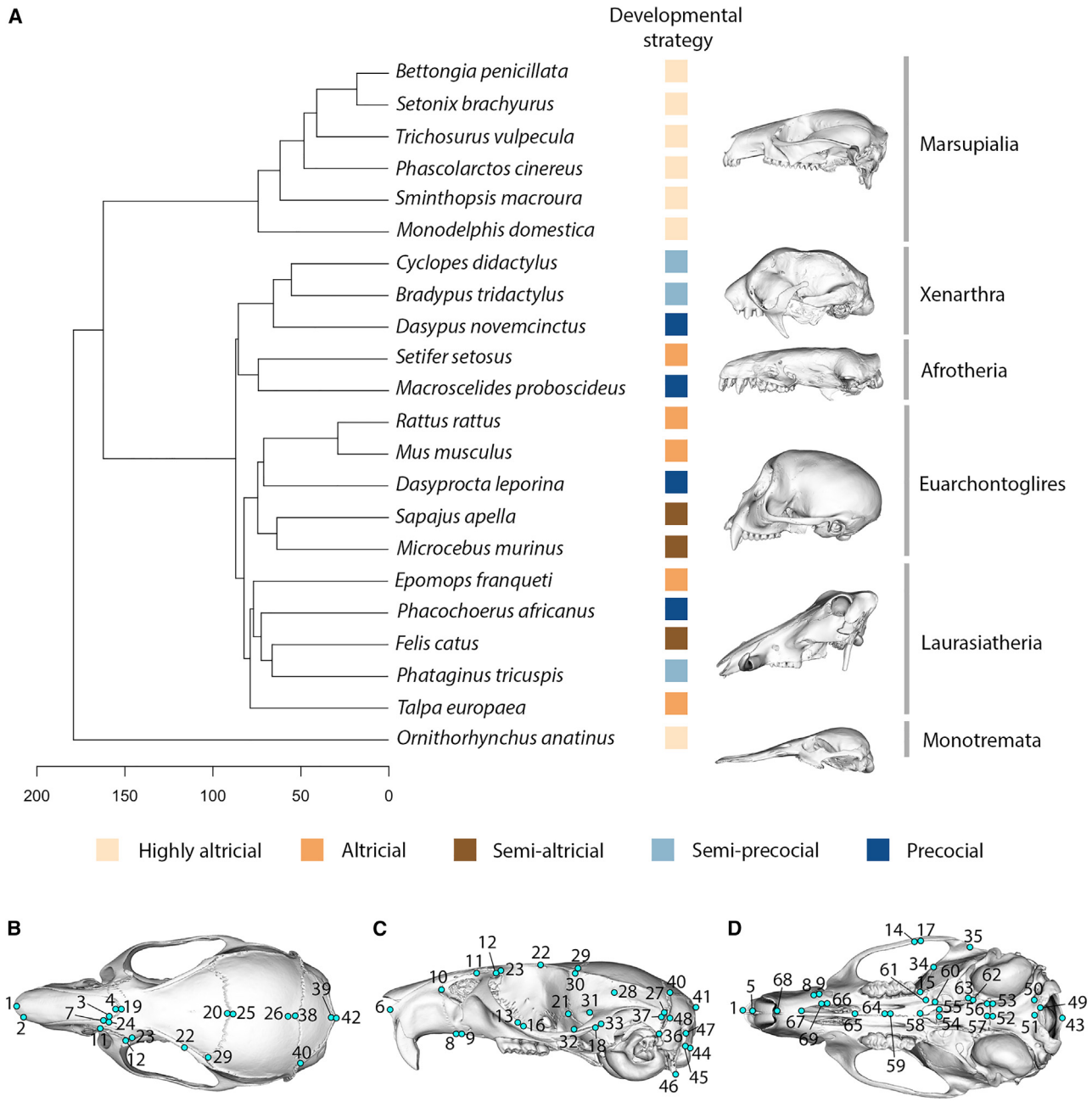

Figure 2. Comparative ontogenetic dataset and morphometric data capture

(A) Phylogenetic relationships of species included within the dataset, based on the phylogeny published by Upham et al.[72]; see also Figure S3 and Tables S1. Timescale is in millions of years. Representatives of major clades, demonstrating the range of cranial morphological diversity, are shown in the lateral view from top to bottom for the following: *Setonix brachyurus*, *Bradypus tridactylus*, *Setifer setosus*, *Sapajus apella*, *Phacochoerus africanus*, and *Ornithorhynchus anatinus*. Developmental strategy for each species is indicated by color; see also Table S1.

(B–D) Landmark positions on *Rattus rattus* skull, relating to descriptions in Table S4. (B) Dorsal view, (C) lateral view, and (D) ventral view.

evolution of mammalian cranial ontogeny and reassess long-standing biases in interpreting the evolution of mammalian development. Our study represents the first quantitative assessment of the role of development and rate heterochrony in cranial evolution across Mammalia, and it sheds new light on the origins of the distinct developmental modes of placental and marsupial mammals.

RESULTS

Cranial mmorphology

A principal-component analysis (PCA) of the adult-only specimens within the dataset (n = 22) was first performed to assess cranial morphological variation captured from the species included in this dataset. The first principal component (PC)

Please cite this article in press as: White et al., Pedomorphosis in the ancestry of marsupial mammals, Current Biology (2023), https://doi.org/10.1016/j.cub.2023.04.009

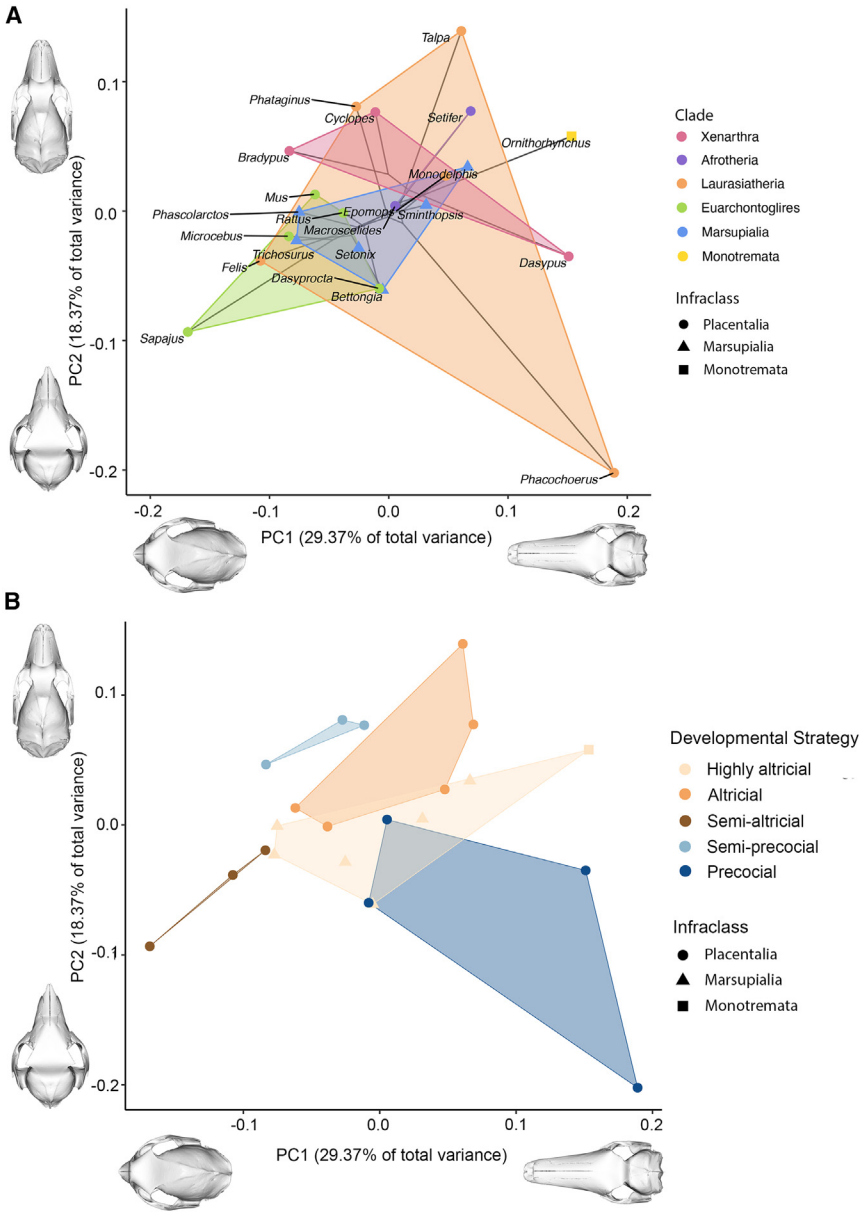

Figure 3. Mammalian cranial morphospace of the adult-only dataset

Morphospace showing estimated warped skull meshes at PC extremes (PC1 and PC2).

(A) Phylomorphospace of the cranial landmark dataset for the adult-only specimens (n = 22) for PC1 and PC2; see also Table S5. Symbol colors indicate clade, and symbol shape indicates infraclass.

(B) Principal-component analysis of the cranial landmark dataset for adult-only specimens (n = 22) for PC1 and PC2. Symbol colors indicate position on the altricial-precocial spectrum (developmental strategy), see also Table S3, and symbol shape indicates infraclass.

explained 29.37% of overall variation and was associated with shape change in rostrum length (Figure 3A; Table S5). The positive end of PC1 reflected an elongated rostrum, exemplified by *Phacochoerus africanus*, *Ornithorhynchus anatinus*, and *Dasypus novemcinctus*. The negative end of PC1 represented the brachycephalic skull morphologies of species such as *Sapajus apella*, *Felis catus*, and *Bradypus tridactylus*. PC2 explained 18.37% of overall variation and predominantly reflected shape change in the cranial vault, in particular the frontal bone. The positive end of PC2 was associated with an elongated, flattened cranial vault, the result of a smaller and more anteriorly positioned frontal bone, as in *Talpa europaea*. The negative end of PC2 represented a rounded cranial vault, with an increased ventral-dorsal height from an enlarged frontal bone (as well as jugal and squamosal bone enlargement), as observed in *Sapajus apella*.

Therian mammal clades (Marsupialia, Xenarthra, Afrotheria, Euarchontoglires, and Laurasiatheria) overlapped extensively in the central region of the PC1-PC2 morphospace (Figure 3A), as would be expected from a PC1-PC2 morphospace and given the diverse sampled dataset. For the taxa sampled within the dataset, placental mammals (n = 15) occupied a larger morphospace area than marsupials (n = 6), although placental mammals were represented by more than double the number of species than marsupials. It is also worth noting the small size of this adult dataset given the developmental focus of the study; therefore, a large proportion of the mammalian morphospace, consisting of approximately 6,000 species, is not sampled here.[73] Of the placental superorders, Laurasiatheria occupied a large region of the morphospace (Procrustes variance [PV] = 0.026), spanning the length of PC1 and PC2 and thus varying greatly in both rostrum length and cranial vault shape. Euarchontoglires were positioned toward the negative end of PC1 (PV = 0.025), mostly displaying a shortened rostrum, but overlapped with Marsupialia in the central region of PC1. *Sapajus apella* deviated most in cranial shape from the other euarchontoglirans. Despite only three species being sampled across Xenarthra and the absence of the unusual *Myrmecophaga* (giant anteater) from the dataset, xenarthran morphospace occupation was large (PV = 0.026). Similarly, Afrotheria presented with high overall disparity (PV = 0.027), which is notable as both Xenarthra and Afrotheria were represented by far fewer species than the less diverse Marsupialia clade (PV = 0.016). Marsupialia occupied a small region of the PC1-PC2 morphospace and had significantly lower morphological disparity than all placental clades (PV = 0.016, $p < 0.01$), despite being represented by several species spanning the phylogenetic breadth of Marsupialia. This marsupial region bridged all other placental mammal superorders. The only monotreme in the dataset (*Ornithorhynchus anatinus*)

Please cite this article in press as: White et al., Pedomorphosis in the ancestry of marsupial mammals, Current Biology (2023), https://doi.org/10.1016/j.cub.2023.04.009

CellPress
OPEN ACCESS

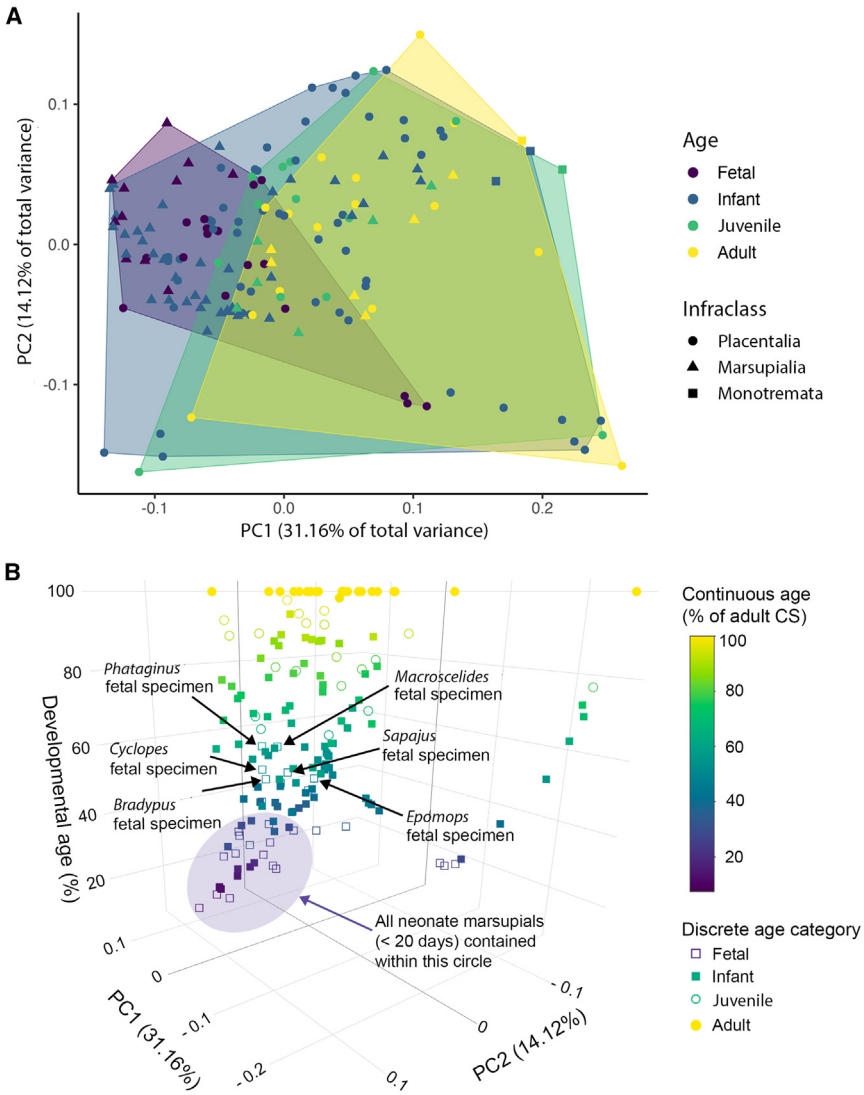

Figure 4. Cranial morphological change through ontogeny

(A) Principal-component analysis of cranial landmarks for the full developmental dataset (n = 165); see also Table S6. Shape indicates infraclass, and color indicates discrete age category.

(B) Principal-component analysis of cranial landmarks for the full developmental dataset (n = 165), plotted against continuous developmental age (percentage of adult size) with discrete age category indicated. Position of the neonatal marsupials is indicated to compare size and shape relative to fetal placentals. Symbol colors indicate age: purple reflects youngest specimens and yellow reflects adults. See also Figures S1 and S2. A 3D version can also be found on the associated GitHub.[74]

falls in the upper right quadrant of the PCA, displaying an elongated rostrum and cranial vault with a small frontal bone. *Ornithorhynchus anatinus* did not overlap in morphospace occupation with any other taxa sampled here, reflecting the unique cranial morphology of this species.

On PC1-PC2, species largely clustered into distinct regions of morphospace based on their position along the altricial-precocial spectrum (divided into five categories from highly altricial to precocial, see STAR Methods, and referred to here as developmental strategy) (Figure 3B). Interestingly, the altricial-precocial spectrum did not appear to align linearly with either PC1 or PC2; highly altricial species clustered centrally along PC1 and PC2, whereas other developmental strategies exhibited more extreme morphologies on these axes. A pMANOVA of shape and developmental strategy (five categories), identified developmental strategy as having a significant and relatively large effect on shape variation, in the adult-only dataset, following allometric and phylogenetic correction ($R^2 = 0.308$, $p = 0.004$). Subdividing the dataset into placental mammals only indicated that species with different developmental strategies (ranging from altricial, semi-altricial, and semi-precocial to precocial in placental mammals) did not overlap in cranial morphospace. Within placentals, developmental strategy was also significantly associated with skull shape after accounting for phylogenetic relationship (pMANOVA: $R^2 = 0.407$, $p < 0.001$).

Cranial morphology across ontogeny

A second PCA, was performed for all specimens within the dataset spanning from fetal to adult stages (n = 165) (Figures 4 and S1). A similar pattern of morphospace occupation to the adult-only PCA (n = 22) was identified, with taxon position remaining largely the same (Figure S1; Table S6). PC1 accounted for 31.16% of overall variation and was associated with change in rostrum length whereas PC2 accounted for 14.12% of overall variation and was associated with shape change in the cranial vault, again dominated by the relative size and position of the frontal bone. All developmental specimens of *Phacochoerus africanus* dominated the bottom right quadrant of the morphospace, which was associated with an elongated rostrum and enlarged frontal bone. *Sapajus apella* dominated the bottom left quadrant (shortened rostrum and rounded cranial vault with an enlarged frontal bone), while *Talpa europaea* occupied the most positive region of PC2 (an elongated cranial vault with an anteriorly positioned, small frontal bone). Greatest taxon overlap occurred toward the negative end of PC1 and the central aspect of PC2, reflecting specimens with shortened, rounded skull morphologies.

Specimens were assigned to four discrete age categories (fetal, infant, juvenile, and adult) based on visual specimen inspection; full details can be found within the STAR Methods. Fetal specimens (purple) clustered at the negative end of PC1 (Figure 4A) and presented with lower levels of disparity (PV = 0.020), compared with juvenile (PV = 0.027) and adult stages (PV = 0.027). This region was associated with shortened,

Please cite this article in press as: White et al., Pedomorphosis in the ancestry of marsupial mammals, Current Biology (2023), https://doi.org/10.1016/j.cub.2023.04.009

rounded skull morphologies. Infant, juvenile, and adult specimens occupied a much larger region of the morphospace, both along PC1 and PC2, demonstrating an increase in morphological diversity (morphospace occupation) with developmental time. Using a continuous metric for age, calculated as the percentage of adult centroid size (relative adult size), to account for potentially inaccurate age assessment in museum collections, similarly indicated a clustering of the youngest specimens (purple) toward the negative end of PC1 and central region of PC2 (Figure S2B). PC1, in particular, was strongly associated with centroid size, often used as proxy of developmental age (R^2 = 0.336, $p < 0.001$). Youngest specimens (relative adult centroid size) (purple) are falling at the negative end, and older specimens (yellow) are sitting at the positive end. Cranial morphologies diversified with developmental age, radiating in both directions on PC2. Across PCs 1 and 2, a clear cone-shaped pattern of cranial shape change through ontogeny was observed when using the continuous age metric (relative adult size) (Figure 4B, a 3D version of this figure can be found on GitHub[74]).

The distribution of specimens across the discrete age categories and the continuous age metric (as estimated by proportion of adult size) were compared on the PCA of all specimens (n = 165) (Figure 4B). As the z axis indicates continuous age (relative adult size), the smallest specimens at the bottom of this axis are, as expected, the small and thus altricial and highly altricial species (including neonate marsupials). In contrast, fetal specimens of some species are relatively larger and more similar in size, relative to their respective adults, than some infant and juvenile specimens of other species. Species with larger fetal specimens are some of the more precocial taxa within the dataset (*Phataginus tricuspis*, *Macroscelides proboscideus*, *Cyclopes didactylus*, and *Bradypus tridactylus*). Consequently, a disconnect between the discrete age categories and relative adult size (continuous age metric) exists, which is linked to position along the altricial-precocial spectrum. Furthermore, developmental strategy (position on the altricial-precocial spectrum) was significantly associated with skull morphology for the full developmental dataset, following allometric correction (R^2 = 0.292, $p < 0.001$).

Allometry and ontogenetic trajectories

The influence of size on multivariate shape was calculated across the full dataset (n = 165). Allometry (size-related shape change) was found to be a significant contributor to overall skull shape variation across all specimens (R^2 = 0.156, $p < 0.001$) and differed significantly across the 22 species (R^2 = 0.070, $p < 0.001$). Multivariate allometry was then compared pairwise across species. A high proportion of significant differences between species' allometries were identified following Bonferroni corrections (77 significant differences from 231 pairwise comparisons, $p < 0.001$; Figure S4A; Table S7). Marsupial taxa showed the greatest number of significant differences, with both placentals and other marsupials, except for *Phascolarctos cinereus*, which showed very few significant differences with other taxa. Both *Phacochoerus africanus* and *Dasypus novemcinctus*, which exhibit elongated rostra, displayed a high number of pairwise significant differences in their allometries. Species with the greatest number of significant differences fall at both extremes of the altricial-precocial spectrum (Figure S4B).

Shape change was also visualized through ontogeny for the major axes of variation (Figure 5), although no statistical analysis was performed for these univariate or PC-specific trajectories, due to issues with univariate analysis of PC axes.[75] For PC1, ontogenetic trajectories for all species followed a similar direction (Figure 5A), progressing from a rounded to a more elongated skull (PC1), although no two species displayed identical trajectories. The species with the steepest trajectories were *Mus musculus* (slope = 0.260) and *Macroscelides proboscideus* (slope = 0.196). *Phascolarctos cinereus* presented with the shallowest slope (slope = 0.038), indicating that this species experienced relatively little skull elongation during ontogeny (although we note that this species showed the fewest significant differences with other species in multivariate allometry, compared with other marsupials). In comparison to other species, the youngest specimens for *Ornithorhynchus anatinus* (yellow) started with an already elongated skull, positioned toward the positive end of PC1. This pattern was also observed in *Phacochoerus africanus*, in which the elongated fetal state largely reflected the adult state of elongation for other species.

Greater variation and divergence were observed for the ontogenetic trajectories of PC2 (Figure 5B), which represented a shape change in the cranial vault (enlargement of the frontal, squamosal, and jugal bones). Approximately half of the sampled species followed a positive slope, while the rest followed a negative slope (Table S8). Most notably, the marsupial species (shown in blue, Figure 5B) followed a similarly shallow negative trajectory for PC2 that differed markedly from all other species (placentals and monotreme). The marsupials generally exhibited a small degree of shape change in the cranial vault through ontogeny, indicating near isometric (scaling) growth for PC2. In contrast, the species with the steepest slope, undergoing the fastest shape change associated with PC2, was the primate *Sapajus apella* (slope = −0.107), while *Sminthopsis macroura* displayed the shallowest slope (slope = 0.003). As with PC1, fetal specimens of *Phacochoerus africanus* displayed similar positions on PC2 to that of adults of other species. For both PC1 and PC2, marsupial species started smaller and presented with the longest trajectories, suggesting hypermorphosis (prolonged growth). While we have only presented figures for ontogenetic trajectories associated with the two largest components of variation, trajectories for all 164 PCs are provided in Table S8.

Ancestral state estimation of cranial shape development

In order to assess evolutionary trends in cranial ontogeny (pedomorphosis and peramorphosis), allometric slopes were estimated for ancestral nodes of the major mammalian lineages and then compared with those of individual species (Figure 1, nodes indicated in Figure S3). Heterochronic shifts were identified by changes in slope and intercept, indicating acceleration and deceleration, as well as pre- and post-displacement, respectively (see STAR Methods for further details). The estimated placental mammal ancestral slope (node 25) was more similar to both the therian mammal (including marsupials and placentals) ancestral slope (node 24) and the crown mammalian (including monotremes and therians) ancestral slope (node 23), compared with that of the marsupials (node 39) (Figure 6A). This result held when ancestral state estimation was performed

Please cite this article in press as: White et al., Pedomorphosis in the ancestry of marsupial mammals, Current Biology (2023), https://doi.org/10.1016/j.cub.2023.04.009

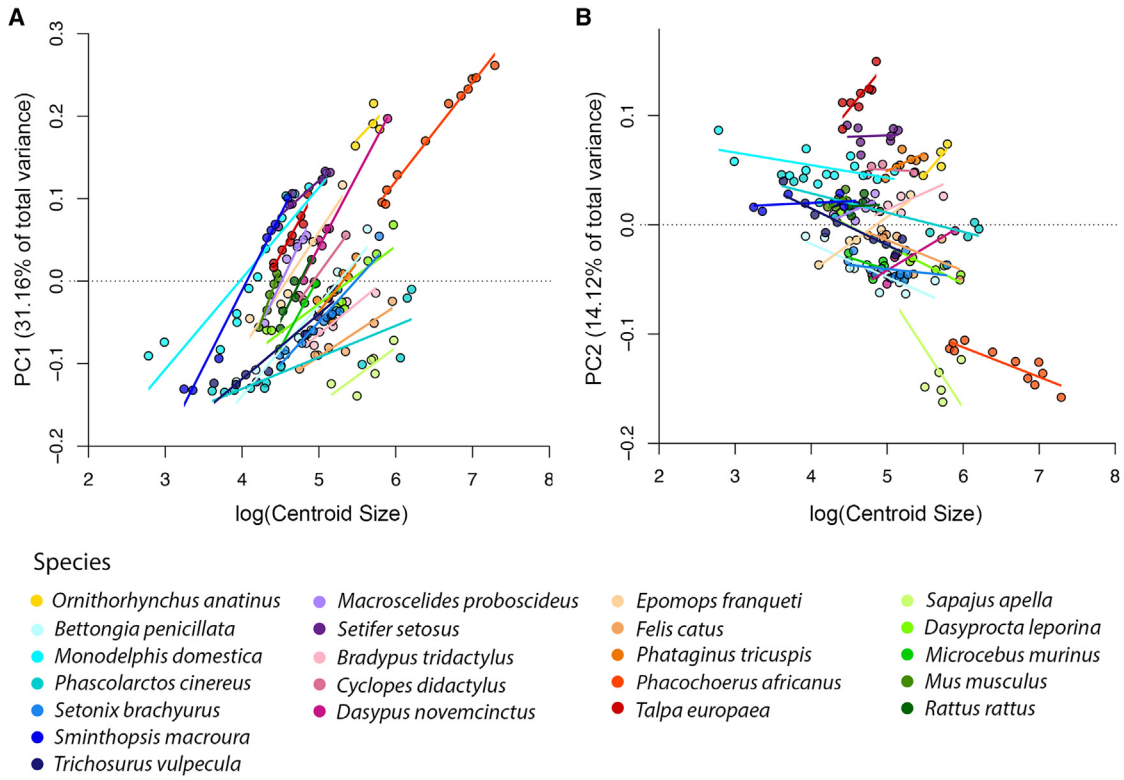

Figure 5. Ontogenetic trajectories for PC1 and PC2

Ontogenetic trajectories for each species (n = 22), associated with PC1 shape change (A) and PC2 shape change (B). Symbol color indicates species. See also Tables S6, S7, and S8 and Figure S4.

on infant, juvenile, and adult specimens only (excluding fetal specimens) due to the lack of early developmental stages for the outgroup taxa (*Ornithorhynchus anatinus*), which may influence ancestral node estimation. Moreover, as estimated values for ancestral states reflect the mean values of tips weighted by phylogenetic distance to the node, the number of taxa used to estimate each node (i.e., marsupials and placentals) may affect ancestral state estimations. Therefore, the placental taxa were subsampled to the same number as the marsupial taxa (n = 6) and analyses were repeated for 1,000 permutations; results of that sensitivity analyses support the observed difference between the ancestral marsupial and ancestral therian (Figure S5D). The sole monotreme in the dataset (*Ornithorhynchus anatinus*) showed both acceleration and post-displacement from the ancestral mammal, although it should be noted that no fetal or early post-natal stages were available for this taxon. The placental and therian mammal ancestral slopes were almost overlaid, with near identical slopes (placental slope = 0.218; therian slope = 0.203). In contrast, the estimated ancestral marsupial presented with a decelerated slope (slope = 0.161) and an earlier onset of growth (pre-displacement), compared with the ancestral therian mammal slope (Figures 6A and S9; Table S9).

All species of marsupial display a small degree of deceleration in comparison to the ancestral marsupial and ancestral mammal estimates, with the exception of *Sminthopsis macroura* that shows slight acceleration in relation to the ancestral marsupial (Figures S5A and S5C; Table S9). *Phascolarctos cinereus* maintained a shallow slope, indicating little shape change through ontogeny (scaling) (Figures S5A and S5C; Table S9). Both a delayed onset of growth (post-displacement) and acceleration were observed for *Ornithorhynchus anatinus* (Figures S5A and S5C; Table S9). Slopes of the xenarthran species were largely similar to the ancestral xenarthran state (Figures S5A and S5C; Table S9). For Afrotheria, *Macroscelides proboscideus* presented a slight degree of acceleration, compared with the ancestral Afrotheria state (Figure S5C; Table S9). Species of both Laurasiatheria and Euarchontoglires displayed greater slope variation, compared with their respective ancestral states (Figure S5A and S5C). *Mus musculus* (Euarchontoglires), which shows the highest slope gradient (highly accelerated green slope on Figure S5C), and *Talpa europaea* (Laurasiatheria) have undergone the greatest degree of acceleration, while *Felis catus* (Laurasiatheria) and *Dasyprocta leporina* (Euarchontoglires) display deceleration in relation to their respective ancestral estimates. Post-displacement (indicated by a lower y intercept) of *Sapajus apella* is observed relative to the ancestral euarchontogliran. A similar pattern of post-displacement was observed for *Phacochoerus africanus* relative to the ancestral laurasiatherian (Figures S5B and S5C; Table S9). All ancestral estimates for each of the four placental superorders were highly aligned with the ancestral placental estimate (Figure 6A). Of the four superorders, the two that displayed the greatest deviation from the ancestral placental estimate were Euarchontoglires and Afrotheria ancestral estimates,

Please cite this article in press as: White et al., Pedomorphosis in the ancestry of marsupial mammals, Current Biology (2023), https://doi.org/10.1016/j.cub.2023.04.009

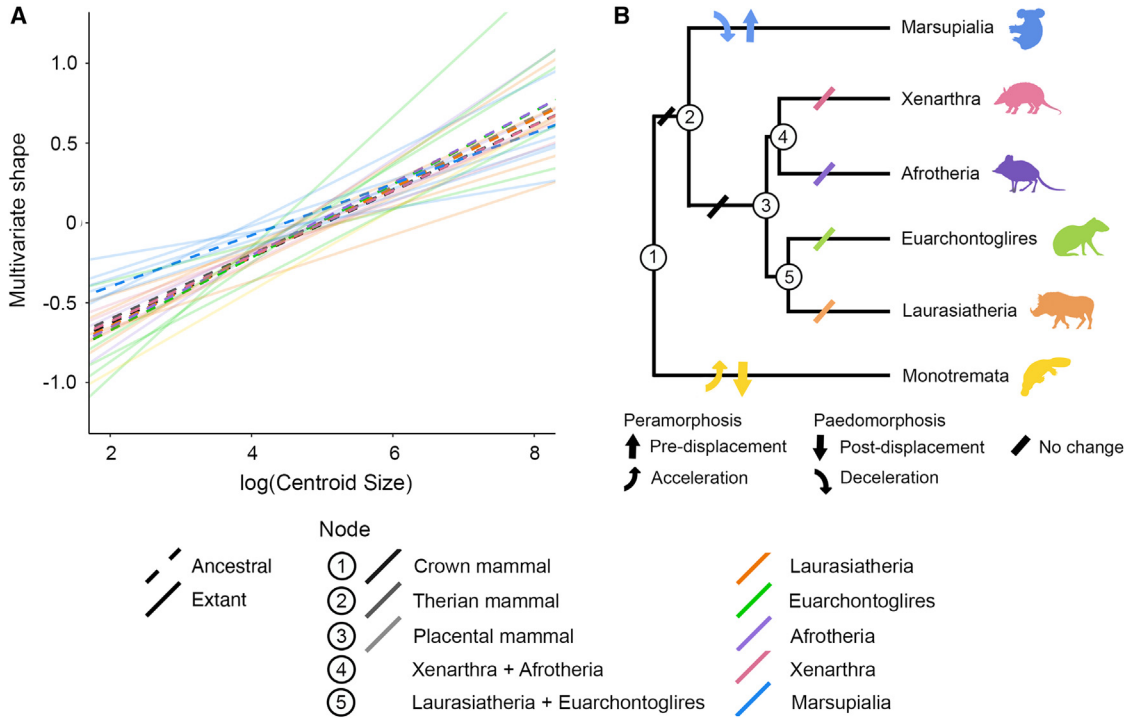

Figure 6. Ancestral state estimations of cranial shape development

(A) Ancestral slopes (dashed regression lines) estimated for the major mammalian nodes (Figure S3) overlying and empirically derived species slopes from multivariate Procrustes regression of multivariate shape and size (transparent solid regression lines) (n = 22). Line colors indicate higher-level clades. See also Tables S7 and S9 and Figures S3 and S5.

(B) Reconstructed heterochronic shifts illustrated for the major mammalian lineages.

both of which indicated slight acceleration, compared with the ancestral placental estimate.

DISCUSSION

Heterochrony is a primary mechanism of evolutionary change. Thus, ascertaining the distribution and polarity of heterochronic shifts across the tree of life is critical for understanding the evolution of morphological diversity. Here, we employed 3D geometric morphometrics to quantify cranial shape change through ontogeny for the largest comparative ontogenetic dataset for mammals to date (22 species, 165 specimens). We identified a morphologically conserved region for fetal specimens, a cone-shaped pattern of cranial development, and a significant impact of the altricial-precocial spectrum (developmental strategy) on cranial morphology across the dataset and for placentals only. Reconstructed ancestral states for cranial shape development demonstrated that pedomorphic shifts localized on the marsupial lineage have resulted in a more derived pattern of cranial development in marsupials than in placentals.

A cone-shaped pattern of development post-ossification

Despite the diversity of cranial morphologies observed across adult specimens, the morphology of fetal specimens falls into a morphologically conserved region of rounded skulls with shortened rostra (Figure 4A). This morphologically conserved developmental period likely coincides with the phylotypic stage hypothesized by the hourglass model,[76,77] which has previously been proposed to occur around the embryo-fetus transition, at the onset of craniofacial ossification.[78,79] While the presence of a morphologically conserved phylotypic stage has been disputed in vertebrates, with one study indicating greater variation at this period,[80] numerous experimental studies across a range of vertebrate taxa have supported its existence.[32,79,81–84] Constraints on morphological diversification, in part due to similar gene expression profiles, are thought to underlie this phylotypic stage or, more generally, morphologically conserved developmental period.[83]

The only fetal specimens to fall outside the highly conserved morphological region were those of *Phacochoerus africanus*. Nevertheless, the morphological variation exhibited across all fetal stages was still substantially smaller than that of the juvenile and adult stages. *Phacochoerus africanus* is the most precocial taxon within the dataset.[9,10] Therefore, the prenatal fetal stages of *Phacochoerus africanus* displayed cranial morphologies more similar to that of their adults, further supported by the similarity in morphospace position of *Phacochoerus africanus* fetal specimens to that of juveniles of other species (Figure 4B).

Across the fetal-to-adult transition, a clear cone-shaped pattern of cranial shape ontogeny is visible and is reflective of the upper half of the developmental hourglass model[76,77] (Figure 7). Phenotypic diversity occurring during the course of ontogeny could be linked to differential rates of bone deposition

Please cite this article in press as: White et al., Pedomorphosis in the ancestry of marsupial mammals, Current Biology (2023), https://doi.org/10.1016/j.cub.2023.04.009

CellPress
OPEN ACCESS

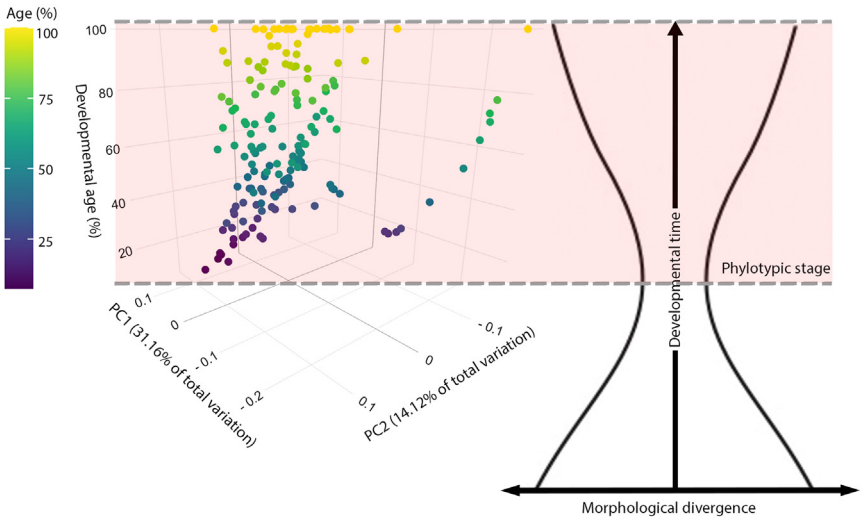

Figure 7. Cone-shaped pattern of cranial morphological development

Cranial morphospace cone-shaped pattern of development reflects the upper half of the developmental hourglass model.[76,77] Data for this PCA are presented in Figure 4B and overlaid with the developmental hourglass model here. See also Figure 4 and Table S6.

and growth along cranial sutures.[85] In contrast, early diversity, reflected by the lower half of the hourglass model, is thought to be driven by developmental mechanisms that occur prior to ossification and bone development, such as organogenesis and neural folding.[79] As our study focused on post-ossification morphology, this earlier ontogenetic diversity was not sampled. Therefore, we cannot test whether the bottom half of the hourglass model, and thus whether the full hourglass model, is supported in this dataset. However, our dataset does provide new understanding of the pace of differentiation following the conserved period of development, with phenotypic diversity established quickly during the infant period. Nevertheless, we do not observe the same ontogenetic changes across the entire skull; in different cranial regions, species follow different ontogenetic changes. For example, all sampled species follow similar ontogenetic trajectories in skull elongation (as captured on PC1) but diverge in the development of the cranial vault (captured on PC2). Interestingly, the neurocranium has been suggested to have a greater degree of developmental lability than the facial region,[86] most likely to support brain growth through development and thereby facilitating evolutionary change.[87–89] Adult phenotypic diversity, arising from this variation in cranial shape across ontogeny, is represented in the uppermost region of the hourglass model.

Given the nature of our dataset, this cone-shaped pattern of development is focused on post-ossification patterns. It is therefore possible that the altricial-precocial spectrum, which has previously been linked to varying rates of ossification, could be linked to species' positioning within the developmental hourglass of cranial shape (Figure 4B). Specifically, the more precocial taxa with increased ossification at birth fall higher along the developmental age axis, whereas the marsupial specimens with highly limited ossification fall toward the smaller end of the developmental age axis, thus experiencing different trajectories through ontogeny. Nevertheless, our data only sample 22 of the approximately 6,000 species of mammal and do not specifically quantify ossification levels. Therefore, further work would be required to elucidate the relationship between the altricial-precocial spectrum and ossification level. As an example of this relationship, not sampled within our dataset, the altricial *Mesocricetus auratus* (golden hamsters) undergoes rapid ossification toward the end of a short gestation period,[90] compared with lengthy cranial ossification during the gestation of the precocial *Loxodonta africana* (African elephant).[91] With further work, it would be interesting to identify whether variation in ossification rate has knock-on implications for specimen position within the cone-shaped pattern of development identified here.

The altricial-precocial spectrum has an underappreciated role in determining skull morphological variation within placentalia

Altriciality and precociality have evolved independently multiple times across placental mammals,[10] resulting in convergent developmental strategies between distantly related species and diverse developmental strategies within each placental superorder. However, the influence of altriciality or precociality on phenotypic evolution has seldom been studied beyond the marsupial-placental boundary,[6,33,46,86] except for works by Zelditch.[92,93] Our results demonstrate that developmental strategy significantly influenced cranial morphological variation through ontogeny and across adults in placentals. Moreover, placentals with different developmental strategies occupy distinct regions of morphospace (Figure 3B), and developmental strategy has a significant influence on cranial shape (R^2 = 0.425, p = 0.002). These results support hypothesized tight coupling of morphology and life history from a study of cranial developmental rate in rodents, spanning from the precocial *Sigmodon fulviventer* to the altricial *Mus musculus domesticus*.[93] It is possible that differing functional requirements at birth for species at different positions on altricial-precocial spectrum (e.g., extended suckling postpartum for the highly altricial marsupials) may act as drivers for the distinct cranial morphologies observed here (Figure 3B).[10] Alternatively, or additionally, variation in gene expression timing and spatial patterning, such as the homeobox genes (e.g., MSx1, Barx1, and Dlx2), which are known to influence cell development in the cranial region,[94,95] could also be involved in generating the observed morphological variation across the altricial-precocial spectrum. Further study is needed to identify the mechanisms behind this morphological variation, but our analyses clearly demonstrate an underappreciated role for the altricial-precocial spectrum in regulating cranial morphological evolution within placentals, and not just between marsupials and placentals.

Please cite this article in press as: White et al., Pedomorphosis in the ancestry of marsupial mammals, Current Biology (2023), https://doi.org/10.1016/j.cub.2023.04.009

As has been previously postulated for species of ungulates[33] and rodents,[93] variation in the degree of maturity at birth may also be reflected by differences observed here in species' allometry (Figure S4B). In rodents, the rate of post-natal development varies with the level of altriciality or precociality. Altricial rodents display a faster rate of post-natal development, due to late ossification during gestation, compared with precocial rodents that undergo slower post-natal development.[93] Of the 77 significant differences in species' pairwise allometries, species displaying the highest proportion of these significant differences were those at the extremes of the altricial-precocial spectrum (highly altricial or precocial) (Figure S4B). Therefore, while positioning on the altricial-precocial spectrum might appear useful for predicting morphology and size of a species at birth, interspecific variation in developmental rate (Figure 6), possibly due to differences in the relative timing of ossification during gestation, complicates the use of neonate maturity or gestation period as accurate indicators of later developmental timings.[93] The relationship between the age, size, and shape of a specimen appeared to be mediated, to some degree, by the respective position of each species on the altricial-precocial spectrum. For example, fetal precocial specimens fell in similar regions of the morphospace to altricial infants (Figure 4B). Our findings support previously proposed hypotheses that ontogenetic regulation of form may be more related to the relative timings of eye opening and weaning (i.e., altriciality and precociality) than to absolute age and that position on the altricial-precocial spectrum may be a stringent regulator of form.[92]

Similarities and differences of mammalian cranial allometries

Shared ontogenetic trajectories have previously been hypothesized to be the result of adaptive responses to convergent ecological niches, as in the marsupial thylacine and placental gray wolf[96] or in blunt-snouted crocodylians.[32] While ontogenetic trajectories follow similar directionality for PC1, there is a large degree of variation across species' allometries, possibly owing to the ecological diversity captured within the dataset. Extensive variation in cranial ontogenetic trajectories has also been reported in other vertebrate systems—such as slender-snouted crocodylians,[32] nightbirds,[43] and mammals[42,96]—and even in closely related species of mammals[97,98] including variation of cranial ontogenetic trajectories between domesticated species and their wild counterparts.[42] Moreover, variation in trajectory length was observed, with marsupials starting smaller and experiencing a prolonged period of growth (hypermorphosis), compared with placentals. This observation of hypermorphosis, or extended post-natal growth, may be expected given that previous studies of marsupials have reported indeterminate or continuous growth,[99,100] as well as extended post-natal growth.[17]

Trajectory divergence was more evident for changes in cranial vault shape, represented on PC2. As discussed above, the cranial vault is thought to display increased developmental lability due to low developmental integration,[86,101] whereas rostrum shape (PC1) has been shown to have a strong allometric signal.[102] This developmental lability is reflected in the extensive divergence of ontogenetic trajectories in cranial vault shape and may enable the cranial vault to respond to changes in brain size across evolutionary and developmental time.[87–89] Marsupials and placentals display marked differences in the level of brain development at birth, which likely influences cranial vault development.[103,104] Brain development in marsupials is delayed relative to that of placentals and occurs predominantly during post-natal growth, in contrast to the early ossification of their oral apparatus.[6,33,45,47,49] Therefore, it is unsurprising that we observe divergence in the ontogenetic trajectories of cranial vault shape for marsupials and placentals. Similarity among marsupial trajectories, as observed here, has previously been associated with high levels of integration that redirect shape change along limited axes of variation, particularly for the early ossifying oral apparatus.[47] Thus, similar ontogenetic trajectories suggest a constrained pattern of marsupial cranial development compared with that of placentals.

Marsupials have the most derived cranial shape development

Marsupials were originally viewed as an evolutionary stepping stone between monotremes and placentals: placentals were originally thought to be derived from marsupials, or more accurately, from an ancestor with marsupial-like development, which in turn were the descendants of an ancestor with monotreme-like development.[14,15] This hypothesis that marsupial developmental mode provides a stepping stone between monotremes and placentals has since been refuted. Instead, the developmental modes of marsupials and placentals are thought to have diverged substantially from their common ancestor.[105,106] However, long-standing biases, held by many authors, have often treated the marsupial developmental strategy as more primitive and more reminiscent of the ancestral therian state than that of placentals,[6,15–18] which is reflected in their total clade names.[19] For example, the immense success of placental mammals, following their adaptive radiation in the wake of the end-Cretaceous mass extinction (66 million years ago),[107–109] has been ascribed to their innovative mode of development, i.e., longer gestation periods supporting more precocial young than their marsupial counterparts.[17,74,110]

While the bias toward viewing marsupial development as primitive has often been seen as a majority view, several opposing studies have argued otherwise.[20,21] In further support of these opposing views, studies have identified components of marsupial craniodental anatomy (dental replacement, dental formula, and auditory modifications) that appear more derived than that of placentals—specifically, the single replacement of metatherian P3/p3[111] and the absence of the primitive stapedial artery system in marsupials.[112] In contrast to the majority view that marsupial development is primitive, but in support of these few opposing studies, we find that ancestral marsupial cranial shape development greatly diverged from that of both the ancestral placental and ancestral therian. The ancestral marsupial displayed a clear signal of pedomorphosis (deceleration) and pre-displacement (Figure 6B), which may be linked to reduced marsupial morphospace occupation and diversity observed here and known marsupial morphological constraint.[46] Our results support the conclusions drawn by the limited dataset of Smith,[21] where it is stated that "the developmental trajectory of all cranial tissues [for marsupials] seems to be shifted." Beyond this heterochronic shift on the marsupial lineage, we

also identified pedomorphosis for *Phacochoerus africanus*, most likely due to its precocial developmental strategy,[9,10] and acceleration for the *Talpa europaea* and *Mus musculus* trajectories. The accelerated growth of *Talpa europaea* may be linked to its rapid ossification of cranial elements,[113] while accelerated growth in *Mus musculus* could be ascribed to its altricial state at birth, as well as its short gestation period.[93,114]

The decelerated pace of marsupial cranial development observed here provides empirical support for the lesser supported hypothesis that marsupial development is more derived than that of placentals.[20,21,111,112] Nevertheless, it is worth highlighting here that due to the difficulties of obtaining ontogenetic data, our dataset, although large, still only represents 22 mammalian species, which are occasionally represented by only four specimens and may result in truncated trajectories. We have highlighted in the results some limitations of the ancestral state estimations, in particular the lack of early developmental stages for *Ornithorhynchus anatinus* and variation in the number of placental and marsupial taxa used to estimate ancestral nodes, although we still identify differences between the ancestral marsupial and the ancestral therian and ancestral placental when these factors are accounted for. Additionally, the nature of this ontogenetic dataset, and the inevitable lack of ontogenetic data for fossils, introduces long phylogenetic branches that may result in inaccurate ancestral state estimations.[115,116] However, based on our result of ancestral marsupial cranial development, we hypothesize that placental mammal cranial ontogeny more closely reflects the condition of the ancestral therian mammal, while the marsupial cranial shape development reflects the most derived state of mammal cranial development, characterized by pedomorphosis. This new understanding provided by our analysis is consistent with a few recent studies, which have suggested that the highly altricial reproductive mode of marsupials is in fact a highly derived state.[117–119] Our hypothesis is further supported by new fossil evidence that precociality evolved early in placental mammals (as in the Palaeocene taxon *Pantolambda bathmodon*).[25] However, while fossil evidence at present suggests that the precocial developmental strategy was established early in placental evolution,[25] we suggest that a more placental-like developmental strategy is more reflective of the ancestral state than is the extreme altriciality of marsupials. As discussed above, placentals display a broad range of developmental strategies, from altricial to highly precocial. However, no placentals are born at the extreme level of altriciality observed in marsupials. Thus, we hypothesize that the ancestral therian mammal displayed a developmental strategy within the range of modern placentals. The extreme altriciality of marsupials thus represents a derived mode of development, rather than a transitional phase between the egg laying monotremes and the more precocial placentals.

More broadly, these results demonstrate that innovations (i.e., the derived pedomorphic marsupial cranial shape development) do not necessarily facilitate the diversification of a clade, counter to the standard implications of the term innovation, given that it is well established that marsupials exhibit less morphological disparity than placentals.[22,46,53] Many questions remain as to the factors and adaptive value that drove the evolution of extreme altriciality in marsupials. Regardless, it is clear that we can no longer consider the marsupial developmental strategy to be a holdover from an intermediate stage of mammal evolution, suggesting that the etymology of the term Metatheria (middle beast) is an inaccurate descriptor of marsupials.

STAR★METHODS

Detailed methods are provided in the online version of this paper and include the following:

- KEY RESOURCES TABLE
- RESOURCE AVAILABILITY
  - Lead contact
  - Materials availability
  - Data and code availability
- EXPERIMENTAL MODEL AND SUBJECT DETAILS
- METHOD DETAILS
  - Characterisation of ontogeny
  - Phylogeny
  - Developmental strategy
  - Morphometric data collection
- QUANTIFICATION AND STATISTICAL ANALYSIS
  - Generalised Procrustes Analysis
  - Cranial morphology
  - Influences on cranial shape
  - Allometry and ontogenetic trajectories
  - Ancestral estimation: Skull shape development

SUPPLEMENTAL INFORMATION

Supplemental information can be found online at https://doi.org/10.1016/j.cub.2023.04.009.

ACKNOWLEDGMENTS

This work was funded by the Biotechnology and Biosciences Research Council through the London Interdisciplinary Doctoral Training Programme (BBSRC LIDo DTP) (grant no. BB/ M009513/1) to H.E.W. CT scan data collection was also supported by the Leverhulme Trust, UK (grant no. F/09364/I) to L.H. and the National Science Foundation (grant nos. NSF 1854469; NSF 2017803) to K.E.S. In addition to our co-authors (L.H., A.H., and K.E.S.), Vera Weisbecker and Robert Asher kindly provided CT data for many marsupial and *Macroscelides proboscideus* specimens, respectively, for this study. Additionally, Jessie Maisano kindly gave access to CT data from MorphoSource. We would also like to thank Anne-Claire Fabre, Ryan Felice, Andrew Knapp, Julien Clavel, Agnese Lanzetti, David Button, Thomas Raven, Carla Bardua, Ellen Coombs, and Eve Noirault, who offered invaluable discussions, methods training, and support with code throughout the process of this study. Thanks also go to R.P.M. and the many other curators and museum staff who enabled access to specimens to compile this dataset. Additional thanks to V.F. and Brett Clark, who helped H.E.W. CT scan the majority of this dataset at NHMUK. Finally, we would like to thank the anonymous reviewers for their thoughtful feedback and comments.

AUTHOR CONTRIBUTIONS

H.E.W., A.G., and A.S.T. conceptualized this research. H.E.W., R.P.M., V.F., L.H., A.H., and K.E.S. acquired the CT data. H.E.W. processed CT data, undertook subsequent data collection, performed analyses, and wrote the initial manuscript. All authors contributed to the discussions and interpretation of data, edited the manuscript, and read and approved the final manuscript version.

DECLARATION OF INTERESTS

The authors declare no competing interests.

Received: February 21, 2023
Revised: February 27, 2023
Accepted: April 5, 2023
Published: April 28, 2023

REFERENCES

1. Benton, M.J., Donoghue, P.C., Vinther, T.J., Asher, R., Friedman, M., Near, T.J., and Vinther, J. (2015). Constraints on the timescale of animal evolutionary history. Palaeontol. Electron. *18*, 1–107. 10.2/JQUERY.MIN.JS.
2. Meredith, R.W., Janečka, J.E., Gatesy, J., Ryder, O.A., Fisher, C.A., Teeling, E.C., Goodbla, A., Eizirik, E., Simão, T.L.L., Stadler, T., et al. (2011). Impacts of the Cretaceous terrestrial revolution and KPg extinction on mammal diversification. Science *334*, 521–524. https://doi.org/10.1126/SCIENCE.1211028/SUPPL_FILE/1211028.MEREDITH.SOM.PDF.
3. Luo, Z.X., Yuan, C.X., Meng, Q.J., and Ji, Q. (2011). A Jurassic eutherian mammal and divergence of marsupials and placentals. Nature *476*, 442–445. https://doi.org/10.1038/nature10291.
4. dos Reis, M., Inoue, J., Hasegawa, M., Asher, R.J., Donoghue, P.C.J., and Yang, Z. (2012). Phylogenomic datasets provide both precision and accuracy in estimating the timescale of placental mammal phylogeny. Proc. Biol. Sci. *279*, 3491–3500. https://doi.org/10.1098/RSPB.2012.0683.
5. Blackburn, D.G. (1999). Viviparity and oviparity: evolution and reproductive strategies. In Encyclopedia of Reproduction, T.E. Knobil, and J.D. Neill, eds. (Academic Press), pp. 994–1003.
6. Lillegraven, J.A. (1975). Biological considerations of the marsupial-placental dichotomy. Evolution *29*, 707–722. https://doi.org/10.2307/2407079.
7. Clough, G.C. (1963). Biology of the arctic shrew, *Sorex arcticus*. Am. Midl. Nat. *69*, 69–81. https://doi.org/10.2307/2422844.
8. Ernest, S.K.M. (2003). Life history characteristics of placental nonvolant mammals. Ecology *84*, 3402. https://doi.org/10.1890/02-9002.
9. Derrickson, E.M. (1992). Comparative reproductive strategies of altricial and precocial eutherian mammals. Funct. Ecol. *6*, 57–65. https://doi.org/10.2307/2389771.
10. Starck, J.M., and Ricklefs, R.E. (1998). Patterns of development: the altricial-precocial spectrum. In Avian Growth and Development, J.M. Starck, and R.E. Ricklefs, eds. (Oxford University Press).
11. Szdzuy, K., Zeller, U., Renfree, M., Tzschentke, B., and Janke, O. (2008). Postnatal lung and metabolic development in two marsupial and four eutherian species. J. Anat. *212*, 164–179. https://doi.org/10.1111/J.1469-7580.2007.00849.X.
12. Smith, K.K., and Keyte, A.L. (2020). Adaptations of the marsupial newborn: birth as an extreme environment. Anat. Rec. (Hoboken) *303*, 235–249. https://doi.org/10.1002/AR.24049.
13. Ferner, K., Schultz, J.A., and Zeller, U. (2017). Comparative anatomy of neonates of the three major mammalian groups (monotremes, marsupials, placentals) and implications for the ancestral mammalian neonate morphotype. J. Anat. *231*, 798–822. https://doi.org/10.1111/JOA.12689.
14. Haekel, E. (1898). The Last Link: Our Present Knowledge of the Descent of Man (Adam and Charles Black).
15. Maier, W. (1993). Cranial morphology of the therian common ancestor, as suggested by the adaptations of neonate marsupials. In Mammal Phylogeny, F.S. Szalay, M.J. Novacek, and M.C. McKenna, eds. (Springer), pp. 165–181. https://doi.org/10.1007/978-1-4615-7381-4_12.
16. Russell, E.M. (1982). Patterns of parental care and parental investment in marsupials. Biol. Rev. Camb. Philos. Soc. *57*, 423–486. https://doi.org/10.1111/J.1469-185X.1982.TB00704.X.
17. Lillegraven, J.A., Thompson, S.D., McNab, B.K., and Patton, J.L. (1987). The origin of eutherian mammals. Biol. J. Linn. Soc. *32*, 281–336. https://doi.org/10.1111/J.1095-8312.1987.TB00434.X.
18. Cooper, W.J., Steppan, S.J., Cooper, W.J., and Steppan, S.J. (2010). Developmental constraint on the evolution of marsupial forelimb morphology. Aust. J. Zool. *58*, 1–15. https://doi.org/10.1071/ZO09102.
19. Huxley, T.H. (1880). On the application of the laws of evolution to the arrangement of the Vertebrata, and more particularly of the Mammalia. Proc. Zool. Soc. Lond. *43*, 649–662.
20. Renfree, M.B. (1993). Ontogeny, genetic control, and phylogeny of female reproduction in monotreme and therian mammals. In Mammal Phylogeny, F.S. Szalay, M.J. Novacek, and M.C. McKenna, eds. (Springer), pp. 4–20. https://doi.org/10.1007/978-1-4613-9249-1_2.
21. Smith, K.K. (2001). The evolution of mammalian development. Bull. Mus. Comp. Zool. *156*, 119–135.
22. Sears, K.E. (2004). Constraints on the morphological evolution of marsupial shoulder girdles. Evolution *58*, 2353–2370. https://doi.org/10.1111/J.0014-3820.2004.TB01609.X.
23. Kelly, E.M.K., and Sears, K.E. (2011). Limb specialization in living marsupial and eutherian mammals: constraints on mammalian limb evolution. J. Mammal. *92*, 1038–1049. https://doi.org/10.1644/10-MAMM-A-425.1.
24. Sánchez-Villagra, M.R., Narita, Y., and Kuratani, S. (2007). Thoracolumbar vertebral number: the first skeletal synapomorphy for afrotherian mammals. Syst. Biodivers. *5*, 1–7. https://doi.org/10.1017/S1477200006002258.
25. Funston, G.F., DePolo, P.E., Sliwinski, J.T., Dumont, M., Shelley, S.L., Pichevin, L.E., Cayzer, N.J., Wible, J.R., Williamson, T.E., Rae, J.W.B., and Brusatte, S.L. (2022). The origin of placental mammal life histories. Nature *610*, 107–111. https://doi.org/10.1038/s41586-022-05150-w.
26. Panciroli, E., Benson, R.B.J., Fernandez, V., Butler, R.J., Fraser, N.C., Luo, Z.-X., and Walsh, S. (2021). New species of mammaliaform and the cranium of *Borealestes* (Mammaliformes: Docodonta) from the Middle Jurassic of the British Isles. Zool. J. Linn. Soc. *192*, 1323–1362. https://doi.org/10.1093/ZOOLINNEAN/ZLAA144.
27. Alberch, P., Gould, S.J., Oster, G.F., and Wake, D.B. (1979). Size and shape in ontogeny and phylogeny. Paleobiology *5*, 296–317. https://doi.org/10.1017/S0094837300006588.
28. Smith, K.K. (2001). Early development of the neural plate, neural crest and facial region of marsupials. J. Anat. *199*, 121–131. https://doi.org/10.1046/J.1469-7580.2001.19910121.X.
29. Smith, K.K. (2003). Time's arrow: heterochrony and the evolution of development. Int. J. Dev. Biol. *47*, 613–621.
30. McNamara, K.J. (2012). Heterochrony: the evolution of development. Evol.: Educ. Outreach *5*, 203–218. https://doi.org/10.1007/S12052-012-0420-3/FIGURES/12.
31. Godoy, P.L., Ferreira, G.S., Montefeltro, F.C., Vila Nova, B.C., Butler, R.J., and Langer, M.C. (2018). Evidence for heterochrony in the cranial evolution of fossil crocodyliforms. Palaeontology *61*, 543–558. https://doi.org/10.1111/PALA.12354.
32. Morris, Z.S., Vliet, K.A., Abzhanov, A., and Pierce, S.E. (2019). Heterochronic shifts and conserved embryonic shape underlie crocodylian craniofacial disparity and convergence. Proc. Biol. Sci. *286*, 20182389. https://doi.org/10.1098/RSPB.2018.2389.
33. Smith, K.K. (1997). Comparative patterns of craniofacial development in eutherian and metatherian mammals. Evolution *51*, 1663–1678. https://doi.org/10.2307/2411218.
34. Smith, K.K. (2002). Sequence heterochrony and the evolution of development. J. Morphol. *252*, 82–97. https://doi.org/10.1002/jmor.10014.
35. Thompson, D.W. (1917). On Growth and Form, First Edition (Cambridge University Press).
36. Klingenberg, C.P. (1998). Heterochrony and allometry: the analysis of evolutionary change in ontogeny. Biol. Rev. Camb. Philos. Soc. *73*, 79–123. https://doi.org/10.1017/S000632319800512X.

37. Zelditch, M.L. (1988). Ontogenetic variation in patterns of phenotypic integration in the laboratory rat. Evolution *42*, 28–41. https://doi.org/10.1111/J.1558-5646.1988.TB04105.X.

38. Zelditch, M.L., Bookstein, F.L., and Lundrigan, B.L. (1992). Ontogeny of integrated skull growth in the cotton rat SIGMODON FULVIVENTER. Evolution *46*, 1164–1180. https://doi.org/10.1111/J.1558-5646.1992.TB00626.X.

39. Gould, S.J. (1966). Allometry and size in ontogeny and phylogeny. Biol. Rev. Camb. Philos. Soc. *41*, 587–640. https://doi.org/10.1111/J.1469-185X.1966.TB01624.X.

40. Lieberman, D.E., Carlo, J., Ponce de León, M., and Zollikofer, C.P.E. (2007). A geometric morphometric analysis of heterochrony in the cranium of chimpanzees and bonobos. J. Hum. Evol. *52*, 647–662. https://doi.org/10.1016/J.JHEVOL.2006.12.005.

41. Bhullar, B.A.S., Marugán-Lobón, J., Racimo, F., Bever, G.S., Rowe, T.B., Norell, M.A., and Abzhanov, A. (2012). Birds have paedomorphic dinosaur skulls. Nature *487*, 223–226. https://doi.org/10.1038/NATURE11146.

42. Wilson, L.A.B. (2018). The evolution of ontogenetic allometric trajectories in mammalian domestication. Evolution *72*, 867–877. https://doi.org/10.1111/EVO.13464.

43. Navalón, G., Nebreda, S.M., Bright, J.A., Fabbri, M., Benson, R.B.J., Bhullar, B.A., Marugán-Lobón, J., and Rayfield, E.J. (2021). Craniofacial development illuminates the evolution of nightbirds (Strisores). Proc. Biol. Sci. *288*, 20210181. https://doi.org/10.1098/RSPB.2021.0181.

44. Smith, K.K. (2006). Craniofacial development in marsupial mammals: developmental origins of evolutionary change. Dev. Dyn. *235*, 1181–1193. https://doi.org/10.1002/DVDY.20676.

45. Weisbecker, V., and Goswami, A. (2010). Brain size, life history, and metabolism at the marsupial/placental dichotomy. Proc. Natl. Acad. Sci. USA *107*, 16216–16221. https://doi.org/10.1073/pnas.0906486107.

46. Bennett, C.V., and Goswami, A. (2013). Statistical support for the hypothesis of developmental constraint in marsupial skull evolution. BMC Biol. *11*, 52. https://doi.org/10.1186/1741-7007-11-52.

47. Goswami, A., Randau, M., Polly, P.D., Weisbecker, V., Bennett, C.V., Hautier, L., and Sánchez-Villagra, M.R. (2016). Do developmental constraints and high integration limit the evolution of the marsupial oral apparatus? Integr. Comp. Biol. *56*, 404–415. https://doi.org/10.1093/ICB/ICW039.

48. Tyndale-Biscoe, H., and Renfree, M.B. (1987). Reproductive Physiology of Marsupials (Cambridge University Press).

49. Nunn, C.L., and Smith, K.K. (1998). Statistical analyses of developmental sequences: the craniofacial region in marsupial and placental mammals. Am. Nat. *152*, 82–101. https://doi.org/10.1086/286151.

50. Schneider, N.Y., and Gurovich, Y. (2017). Morphology and evolution of the oral shield in marsupial neonates including the newborn monito del monte (*Dromiciops gliroides*, marsupialia Microbiotheria) pouch young. J. Anat. *231*, 59–83. https://doi.org/10.1111/JOA.12621.

51. Spiekman, S.N.F., and Werneburg, I. (2017). Patterns in the bony skull development of marsupials: high variation in onset of ossification and conserved regions of bone contact. Sci. Rep. *7*, 43197. https://doi.org/10.1038/srep43197.

52. Fabre, A.C., Dowling, C., Portela Miguez, R., Fernandez, V., Noirault, E., and Goswami, A. (2021). Functional constraints during development limit jaw shape evolution in marsupials. Proc. Biol. Sci. *288*, 20210319. https://doi.org/10.1098/RSPB.2021.0319.

53. Prevosti, F.J., Turazzini, G.F., Ercoli, M.D., and Hingst-Zaher, E. (2012). Mandible shape in marsupial and placental carnivorous mammals: a morphological comparative study using geometric morphometrics. Zool. J. Linn. Soc. *164*, 836–855. https://doi.org/10.1111/J.1096-3642.2011.00785.X.

54. Sánchez-Villagra, M.R. (2013). Why are there fewer marsupials than placentals? On the relevance of geography and physiology to evolutionary patterns of mammalian diversity and disparity. J. Mammal. Evol. *20*, 279–290. https://doi.org/10.1007/S10914-012-9220-3/FIGURES/1.

55. Goswami, A., Milne, N., and Wroe, S. (2011). Biting through constraints: cranial morphology, disparity and convergence across living and fossil carnivorous mammals. Proc. Biol. Sci. *278*, 1831–1839. https://doi.org/10.1098/RSPB.2010.2031.

56. Garland, K., Marcy, A., Sherratt, E., and Weisbecker, V. (2017). Out on a limb: bandicoot limb co-variation suggests complex impacts of development and adaptation on marsupial forelimb evolution. Evol. Dev. *19*, 69–84. https://doi.org/10.1111/EDE.12220.

57. Martín-Serra, A., and Benson, R.B.J. (2020). Developmental constraints do not influence long-term phenotypic evolution of marsupial forelimbs as revealed by interspecific disparity and integration patterns. Am. Nat. *195*, 547–560. https://doi.org/10.1086/707194.

58. Scheiber, I.B.R., Weiß, B.M., Kingma, S.A., and Komdeur, J. (2017). The importance of the altricial – precocial spectrum for social complexity in mammals and birds – a review. Front. Zool. *14*, 3. https://doi.org/10.1186/S12983-016-0185-6.

59. Coombs, E.J., Felice, R.N., Clavel, J., Park, T., Bennion, R.F., Churchill, M., Geisler, J.H., Beatty, B., and Goswami, A. (2022). The tempo of cetacean cranial evolution. Curr. Biol. *32*. 2233.e4-2247.e4. https://doi.org/10.1016/J.CUB.2022.04.060.

60. Goswami, A. (2006). Cranial modularity shifts during mammalian evolution. Am. Nat. *168*, 270–280. https://doi.org/10.1086/505758.

61. Gunz, P., Mitteroecker, P., Neubauer, S., Weber, G.W., and Bookstein, F.L. (2009). Principles for the virtual reconstruction of hominin crania. J. Hum. Evol. *57*, 48–62. https://doi.org/10.1016/J.JHEVOL.2009.04.004.

62. Lu, X., Ge, D., Xia, L., Huang, C., and Yang, Q. (2014). Geometric morphometric study of the skull shape diversification in Sciuridae (Mammalia, Rodentia). Integr. Zool. *9*, 231–245. https://doi.org/10.1111/1749-4877.12035.

63. Dumont, M., Wall, C.E., Botton-Divet, L., Goswami, A., Peigné, S., and Fabre, A.C. (2016). Do functional demands associated with locomotor habitat, diet, and activity pattern drive skull shape evolution in musteloid carnivorans? Biol. J. Linn. Soc. *117*, 858–878. https://doi.org/10.1111/BIJ.12719.

64. Randau, M., Sanfelice, D., and Goswami, A. (2019). Shifts in cranial integration associated with ecological specialization in pinnipeds (Mammalia, Carnivora). R. Soc. Open Sci. *6*, 190201. https://doi.org/10.1098/RSOS.190201.

65. Goswami, A., and Prochel, J. (2007). Ontogenetic morphology and allometry of the cranium in the common European mole (*Talpa europaea*). J. Mammal. *88*, 667–677. https://doi.org/10.1644/06-MAMM-A-315R.1.

66. Herrel, A., Fabre, A.C., Hugot, J.P., Keovichit, K., Adriaens, D., Brabant, L., van Hoorebeke, L., and Cornette, R. (2012). Ontogeny of the cranial system in *Laonastes aenigmamus*. J. Anat. *221*, 128–137. https://doi.org/10.1111/J.1469-7580.2012.01519.X.

67. Camacho, J., Heyde, A., Bhullar, B.S., Haelewaters, D., Simmons, N.B., and Abzhanov, A. (2019). Peramorphosis, an evolutionary developmental mechanism in Neotropical bat skull diversity. Dev. Dyn. *248*, 1129–1143. https://doi.org/10.1002/DVDY.90.

68. Heck, L., Sanchez-Villagra, M.R., and Stange, M. (2019). Why the long face? Comparative shape analysis of miniature, pony, and other horse skulls reveals changes in ontogenetic growth. PeerJ *7*, e7678. https://doi.org/10.7717/PEERJ.7678.

69. Geiger, M., Evin, A., Sánchez-Villagra, M.R., Gascho, D., Mainini, C., and Zollikofer, C.P.E. (2017). Neomorphosis and heterochrony of skull shape in dog domestication. Sci. Rep. *7*, 13443. https://doi.org/10.1038/s41598-017-12582-2.

70. Tanner, J.B., Zelditch, M.L., Lundrigan, B.L., and Holekamp, K.E. (2010). Ontogenetic change in skull morphology and mechanical advantage in the spotted hyena (*Crocuta crocuta*). J. Morphol. *271*, 353–365. https://doi.org/10.1002/JMOR.10802.

71. Giannini, N.P., Segura, V., Giannini, M.I., and Flores, D. (2010). A quantitative approach to the cranial ontogeny of the puma. Mamm. Biol. *75*, 547–554. https://doi.org/10.1016/J.MAMBIO.2009.08.001.

72. Upham, N.S., Esselstyn, J.A., and Jetz, W. (2019). Inferring the mammal tree: species-level sets of phylogenies for questions in ecology, evolution, and conservation. PLoS Biol. *17*, e3000494. https://doi.org/10.1371/JOURNAL.PBIO.3000494.

73. Goswami, A., Noirault, E., Coombs, E.J., Clavel, J., Fabre, A.C., Halliday, T.J.D., Churchill, M., Curtis, A., Watanabe, A., Simmons, N.B., et al. (2022). Attenuated evolution of mammals through the Cenozoic. Science *378*, 377–383. https://doi.org/10.1126/science.abm7525.

74. Thompson, S.D. (1987). Body size, duration of parental care, and the intrinsic rate of natural increase in eutherian and metatherian mammals. Oecologia *71*, 201–209. https://doi.org/10.1007/BF00377285.

75. Uyeda, J.C., Caetano, D.S., and Pennell, M.W. (2015). Comparative analysis of principal components can be misleading. Syst. Biol. *64*, 677–689. https://doi.org/10.1093/SYSBIO/SYV019.

76. Duboule, D. (1994). Temporal colinearity and the phylotypic progression: a basis for the stability of a vertebrate Bauplan and the evolution of morphologies through heterochrony. Development, 135–142.

77. Raff, R.A. (1996). The Shape of Life: Genes, Development, and the Evolution of Animal Form (University of Chicago Press). https://doi.org/10.1086/419892.

78. Young, N.M., Hu, D., Lainoff, A.J., Smith, F.J., Diaz, R., Tucker, A.S., Trainor, P.A., Schneider, R.A., Hallgrímsson, B., and Marcucio, R.S. (2014). Embryonic Bauplans and the developmental origins of facial diversity and constraint. Development *141*, 1059–1063. https://doi.org/10.1242/DEV.099994.

79. Cordero, G.A., Sánchez-Villagra, M.R., and Werneburg, I. (2020). An irregular hourglass pattern describes the tempo of phenotypic development in placental mammal evolution. Biol. Lett. *16*, 20200087. https://doi.org/10.1098/RSBL.2020.0087.

80. Bininda-Emonds, O.R.P., Jeffery, J.E., and Richardson, M.K. (2003). Inverting the hourglass: quantitative evidence against the phylotypic stage in vertebrate development. Proc. Biol. Sci. *270*, 341–346. https://doi.org/10.1098/RSPB.2002.2242.

81. Hazkani-Covo, E., Wool, D., and Graur, D. (2005). In search of the vertebrate phylotypic stage: a molecular examination of the developmental hourglass model and von Baer's third law. J. Exp. Zool. B Mol. Dev. Evol. *304*, 150–158. https://doi.org/10.1002/JEZ.B.21033.

82. Liu, B., Rooker, S.M., and Helms, J.A. (2010). Molecular control of facial morphology. Semin. Cell Dev. Biol. *21*, 309–313. https://doi.org/10.1016/J.SEMCDB.2009.09.002.

83. Irie, N., and Kuratani, S. (2011). Comparative transcriptome analysis reveals vertebrate phylotypic period during organogenesis. Nat. Commun. *2*, 248. https://doi.org/10.1038/ncomms1248.

84. Levin, M., Anavy, L., Cole, A.G., Winter, E., Mostov, N., Khair, S., Senderovich, N., Kovalev, E., Silver, D.H., Feder, M., et al. (2016). The mid-developmental transition and the evolution of animal body plans. Nature *531*, 637–641. https://doi.org/10.1038/nature16994.

85. White, H.E., Goswami, A., and Tucker, A.S. (2021). The intertwined evolution and development of sutures and cranial morphology. Front. Cell Dev. Biol. *9*, 653579. https://doi.org/10.3389/FCELL.2021.653579/XML/NLM.

86. Sánchez-Villagra, M.R., Goswami, A., Weisbecker, V., Mock, O., and Kuratani, S. (2008). Conserved relative timing of cranial ossification patterns in early mammalian evolution. Evol. Dev. *10*, 519–530. https://doi.org/10.1111/j.1525-142X.2008.00267.x.

87. Luo, Z.X., Crompton, A.W., and Sun, A.L. (2001). A new mammaliaform from the Early Jurassic and evolution of mammalian characteristics. Science *292*, 1535–1540. https://doi.org/10.1126/science.1058476.

88. Richtsmeier, J.T., and Flaherty, K. (2013). Hand in glove: brain and skull in development and dysmorphogenesis. Acta Neuropathol. *125*, 469–489. https://doi.org/10.1007/S00401-013-1104-Y.

89. Koyabu, D., Werneburg, I., Morimoto, N., Zollikofer, C.P.E., Forasiepi, A.M., Endo, H., Kimura, J., Ohdachi, S.D., Truong Son, N., and Sánchez-Villagra, M.R. (2014). Mammalian skull heterochrony reveals modular evolution and a link between cranial development and brain size. Nat. Commun. *5*, 3625. https://doi.org/10.1038/ncomms4625.

90. Kanazawa, E., and Mochizuki, K. (1974). The time and order of appearance of ossification centers in the hamster before birth. Jikken Dobutsu *23*, 113–122. https://doi.org/10.1538/EXPANIM1957.23.3_113.

91. Hautier, L., Stansfield, F.J., Allen, W.R., and Asher, R.J. (2012). Skeletal development in the African elephant and ossification timing in placental mammals. Proc. Biol. Sci. *279*, 2188–2195. https://doi.org/10.1098/RSPB.2011.2481.

92. Zelditch, M.L., Bookstein, F.L., and Lundrigan, B.L. (1993). The ontogenetic complexity of developmental constraints. J. Evol. Biol. *6*, 621–641. https://doi.org/10.1046/j.1420-9101.1993.6050621.x.

93. Zelditch, M.L., Lundrigan, B.L., Sheets, H.D., and Garland, T. (2003). Do precocial mammals develop at a faster rate? A comparison of rates of skull development in *Sigmodon fulviventer* and *Mus musculus domesticus*. J. Evol. Biol. *16*, 708–720. https://doi.org/10.1046/J.1420-9101.2003.00568.X.

94. Alappat, S., Zhang, Z.Y., and Chen, Y.P. (2003). Msx homeobox gene family and craniofacial development. Cell. Res. *13*, 429–442. https://doi.org/10.1038/sj.cr.7290185.

95. Sumiyama, K., Miyake, T., Grimwood, J., Stuart, A., Dickson, M., Schmutz, J., Ruddle, F.H., Myers, R.M., and Amemiya, C.T. (2012). Theria-specific homeodomain and cis-regulatory element evolution of the Dlx3-4 bigene cluster in 12 different mammalian species. J. Exp. Zool. B Mol. Dev. Evol. *318*, 639–650. https://doi.org/10.1002/JEZ.B.22469.

96. Newton, A.H., Weisbecker, V., Pask, A.J., and Hipsley, C.A. (2021). Ontogenetic origins of cranial convergence between the extinct marsupial thylacine and placental gray wolf. Commun. Biol. *4*, 51. https://doi.org/10.1038/s42003-020-01569-x.

97. O'Higgins, P., Chadfield, P., and Jones, N. (2001). Facial growth and the ontogeny of morphological variation within and between the primates *Cebus apella* and *Cercocebus torquatus*. J. Zool. *254*, 337–357. https://doi.org/10.1017/S095283690100084X.

98. Singleton, M. (2002). Patterns of cranial shape variation in the Papionini (Primates: Cercopithecinae). J. Hum. Evol. *42*, 547–578. https://doi.org/10.1006/JHEV.2001.0539.

99. Read, D.G. (1987). The von Bertalanffy growth model fitted to *Planigale tenuirostris* (marsupialia: Dasyuridae) post-weaning data. J. Zool. *212*, 1–5. https://doi.org/10.1111/J.1469-7998.1987.TB05110.X.

100. Cockburn, A., and Johnson, C.N. (1988). Patterns of growth. In The Developing Marsupial (Springer), pp. 28–40. https://doi.org/10.1007/978-3-642-88402-3_3.

101. Goswami, A. (2007). Cranial modularity and sequence heterochrony in mammals. Evol. Dev. *9*, 290–298. https://doi.org/10.1111/j.1525-142X.2007.00161.x.

102. Gomes Rodrigues, H.G., Cornette, R., Clavel, J., Cassini, G., Bhullar, B.S., Fernández-Monescillo, M., Moreno, K., Herrel, A., and Billet, G. (2018). Differential influences of allometry, phylogeny and environment on the rostral shape diversity of extinct South American notoungulates. R. Soc. Open Sci. *5*, 171816. https://doi.org/10.1098/RSOS.171816.

103. Young, R.W. (1959). The influence of cranial contents on postnatal growth of the skull in the rat. Am. J. Anat. *105*, 383–415. https://doi.org/10.1002/AJA.1001050304.

104. Smith, D.W., and Töndury, G. (1978). Origin of the calvaria and its sutures. Am. J. Dis. Child. *132*, 662–666. https://doi.org/10.1001/ARCHPEDI.1978.02120320022004.

105. Zeller, U., and Freyer, C. (2001). Early ontogeny and placentation of the grey short-tailed opossum, *Monodelphis domestica* (Didelphidae: marsupialia): contribution to the reconstruction of the marsupial morphotype.

J. Zool. Syst. Evol. Res. *39*, 137–158. https://doi.org/10.1046/J.1439-0469.2001.00167.X.

106. Freyer, C., Zeller, U., and Renfree, M.B. (2003). The marsupial placenta: a phylogenetic analysis. J. Exp. Zool. A Comp. Exp. Biol. *299*, 59–77. https://doi.org/10.1002/JEZ.A.10291.

107. Alroy, J. (1998). Cope's rule and the dynamics of body mass evolution in North American fossil mammals. Science *280*, 731–734. https://doi.org/10.1126/SCIENCE.280.5364.731.

108. Bininda-Emonds, O.R.P., Cardillo, M., Jones, K.E., MacPhee, R.D.E., Beck, R.M.D., Grenyer, R., Price, S.A., Vos, R.A., Gittleman, J.L., and Purvis, A. (2007). The delayed rise of present-day mammals. Nature *446*, 507–512. https://doi.org/10.1038/nature05634.

109. Halliday, T.J.D., and Goswami, A. (2016). Eutherian morphological disparity across the end-Cretaceous mass extinction. Biol. J. Linn. Soc. *118*, 152–168. https://doi.org/10.1111/BIJ.12731.

110. Kiltie, R.A. (1984). Seasonality, gestation time, and large mammal extinctions. In Quaternary Extinctions: a Prehistoric Revolution, P.S. Martin, and R.G. Klrin, eds. (The University of Arizona Press), pp. 299–314. https://doi.org/10.2307/j.ctv264f91j.20.

111. Luo, Z.-X., Kielan-Jaworowska, Z., and Cifelli, R.L. (2004). Evolution of dental replacement in mammals. Bull. Carnegie Mus. Nat. Hist. *36*, 159–175.

112. Rougier, G., and Wible, J.R. (2006). Major changes in the ear region and basicranium of early mammals. In Amniote Paleobiology: Perspectives on the Evolution of Mammals, Birds, and Reptiles, M. Carrano, T. Gaudin, R. Blob, and J. Wible, eds. (Chicago University Press), pp. 269–311.

113. Prochel, J., Goswami, A., David Carmona, F., and Jimenéz, R. (2008). Ossification sequence in the mole *Talpa occidentalis* (Eulipotyphla, Talpidae) and comparison with other mammals. Mamm. Biol. *73*, 399–403. https://doi.org/10.1016/J.MAMBIO.2007.05.014.

114. Willmore, K.E., Leamy, L., and Hallgrímsson, B. (2006). Effects of developmental and functional interactions on mouse cranial variability through late ontogeny. Evol. Dev. *8*, 550–567. https://doi.org/10.1111/j.1525-142X.2006.00127.x.

115. Litsios, G., and Salamin, N. (2012). Effects of phylogenetic signal on ancestral state reconstruction. Syst. Biol. *61*, 533–538. https://doi.org/10.1093/SYSBIO/SYR124.

116. Salisbury, B.A.S., and Kim, J. (2001). Ancestral state estimation and taxon sampling density. Syst. Biol. *50*, 557–564. https://doi.org/10.1080/10635150119819.

117. Hayssen, V., Lacy, R.C., and Parker, P.J. (1985). Metatherian reproduction: transitional or transcending? Am. Nat. *126*, 617–632. https://doi.org/10.1086/284443.

118. Smith, K.K. (2015). Placental evolution in therian mammals. In Great Transformations in Vertebrate Evolution, K.P. Dial, N. Shubin, and E.L. Brainerd, eds. (University of Chicago Press).

119. Weaver, L.N., Fulghum, H.Z., Grossnickle, D.M., Brightly, W.H., Kulik, Z.T., Wilson Mantilla, G.P., and Whitney, M.R. (2022). Multituberculate mammals show evidence of a life history strategy similar to that of placentals, not marsupials. Am. Nat. *200*, 383–400. https://doi.org/10.1086/720410.

120. Clavel, J., Merceron, G., and Escarguel, G. (2014). Missing data estimation in morphometrics: how much is too much? Syst. Biol. *63*, 203–218. https://doi.org/10.1093/SYSBIO/SYT100.

121. White, H.E., and Goswami, A. (2023). Paedomorphosis at the origin of marsupial mammals Github. https://github.com/HeatherEWhite/mammal_cranial_development.

122. Jin, S.W., Sim, K.B., and Kim, S.D. (2016). Development and growth of the normal cranial vault: an embryologic review. J. Korean Neurosurg. Soc. *59*, 192–196. https://doi.org/10.3340/JKNS.2016.59.3.192.

123. Cignoni, P., Corsini, M., and Ranzuglia, G. (2008). Meshlab: an open-source 3d mesh processing system. ERCIM News *73*, 47–48.

124. Bardua, C., Felice, R.N., Watanabe, A., Fabre, A.C., and Goswami, A. (2019). A practical guide to sliding and surface semilandmarks in morphometric analyses. Integr. Org. Biol. *1*, obz016. https://doi.org/10.1093/IOB/OBZ016.

125. Zelditch, M., Swiderski, D., and Sheets, H. (2012). Geometric Morphometrics for Biologists (Academic Press). https://doi.org/10.1016/C2010-0-66209-2.

126. Paradis, E., Claude, J., and Strimmer, K. (2004). APE: analyses of phylogenetics and evolution in R language. Bioinformatics *20*, 289–290. https://doi.org/10.1093/BIOINFORMATICS/BTG412.

127. Beck, R.M.D., Voss, R.S., and Jansa, S.A. (2022). Craniodental morphology and phylogeny of marsupials. Bull. Am. Mus. Nat. Hist. *457*, 1–350.

128. Bookstein, F.L. (1991). Morphometric Tools for Landmark Data: Geometry and Biology (Cambridge University Press).

129. Bookstein, F.L. (1997). Landmark methods for forms without landmarks: morphometrics of group differences in outline shape. Med. Image Anal. *1*, 225–243. https://doi.org/10.1016/S1361-8415(97)85012-8.

130. Johnson, M.L. (1933). The time and order of appearance of ossification centers in the albino mouse. Am. J. Anat. *52*, 241–271. https://doi.org/10.1002/AJA.1000520203.

131. Adler, D., and Murdoch, D. (2007). Rgl: 3D visualization device system (OpenGL). R package version 0.75. http://rgl.neoscientists.org.

132. Adams, D.C., and Otárola-Castillo, E. (2013). Geomorph: an R package for the collection and analysis of geometric morphometric shape data. Methods Ecol. Evol. *4*, 393–399. https://doi.org/10.1111/2041-210X.12035.

133. Koyabu, D., Maier, W., and Sánchez-Villagra, M.R. (2012). Paleontological and developmental evidence resolve the homology and dual embryonic origin of a mammalian skull bone, the interparietal. Proc. Natl. Acad. Sci. USA *109*, 14075–14080. https://doi.org/10.1073/pnas.1208693109.

134. R Core Team (2019). R: A Language and Environment for Statistical Computing (R Foundation for Statistical Computing).

135. Gower, J.C. (1975). Generalized Procrustes analysis. Psychometrika *40*, 33–51. https://doi.org/10.1007/BF02291478.

136. Rohlf, F.J., and Slice, D. (1990). Extensions of the Procrustes method for the optimal superimposition of landmarks. Syst. Zool. *39*, 40–59. https://doi.org/10.2307/2992207.

137. Cardini, A. (2016). Lost in the other half: improving accuracy in geometric morphometric analyses of one side of bilaterally symmetric structures. Syst. Biol. *65*, 1096–1106. https://doi.org/10.1093/SYSBIO/SYW043.

138. Cardini, A. (2017). Left, right or both? Estimating and improving accuracy of one-side-only geometric morphometric analyses of cranial variation. J. Zool. Syst. Evol. Res. *55*, 1–10. https://doi.org/10.1111/JZS.12144.

139. Revell, L.J. (2012). Phytools: an R package for phylogenetic comparative biology (and other things). Methods Ecol. Evol. *3*, 217–223. https://doi.org/10.1111/j.2041-210X.2011.00169.x.

140. Lanzetti, A., Coombs, E.J., Portela Miguez, R.P., Fernandez, V., and Goswami, A. (2022). The ontogeny of asymmetry in echolocating whales. Proc. Biol. Sci. *289*, 20221090. https://doi.org/10.1098/RSPB.2022.1090.

Please cite this article in press as: White et al., Pedomorphosis in the ancestry of marsupial mammals, Current Biology (2023), https://doi.org/10.1016/j.cub.2023.04.009

STAR★METHODS

KEY RESOURCES TABLE

REAGENT or RESOURCE	SOURCE	IDENTIFIER
Deposited data		
Trees for all phylogenetic analyses	https://github.com/HeatherEWhite/mammal_cranial_development White and Goswami[121] Upham et al.[72]	N/A
MicroCT scans	https://www.phenome10k.org/	N/A
Software and algorithms		
R Studio v. 3.6.1	R Core Team[134]	N/A
Code for all analyses	https://github.com/HeatherEWhite/mammal_cranial_development White and Goswami[121]	N/A

RESOURCE AVAILABILITY

Lead contact

Further information and requests for resources should be directed to and will be fulfilled by the lead contact, Heather White (h.white@nhm.ac.uk).

Materials availability

3D scan data available at: https://www.morphosource.org/. To be made publicly available when accepted.

Data and code availability

All original code is available at a public GitHub repository.[121] All code and raw data are available to download, complete with MIT license. Please cite this paper and the Zenodo https://doi.org/10.5281/zenodo.7850303 when using the data or raw code. Further details are listed in the key resources table. All R package version details available at: https://github.com/HeatherEWhite/mammal_cranial_development.

EXPERIMENTAL MODEL AND SUBJECT DETAILS

The comparative dataset comprises 22 species that span the phylogenetic breadth of Mammalia including representatives of the four major placental superorders (Xenarthra, Afrotheria, Laurasiatheria, and Euarchontoglires), the three most diverse marsupial orders (Didelphimorphia, Dasyuromorphia, and Diprotodontia), and Monotremata (Table S1; Figure 1A). For each of the species, multiple developmental stages were collected, in most cases ranging from fetus to adult, with from 4–13 specimens per species (total: n=165; adults: n=22), to produce the largest three-dimensional comparative ontogenetic framework for Mammalia to date (Table S1). Specimens within the ontogenetic dataset were limited to those with at least 75% of the total number of cranial bones present, which balances the need for inclusion of fetal specimens with a reduction of missing data, although it necessarily excludes earlier embryonic stages with little cranial ossification. By limiting specimens to fetal stages with more than 75% of cranial bone present, this reduced the quantity of missing geometric morphometric data, which can be problematic in morphological analyses.[120] This requirement resulted in the dataset capturing only fetal specimens that have undergone prenatal cranial ossification,[122] whilst also reducing the quantity of missing geometric morphometric data (see below for details on treatment of missing morphometric data). Therefore, several fetal specimens were excluded from the dataset (n=7), reducing the dataset to 165 specimens. Further details on the characterisation of ontogeny can be found below. Specimens were collected from global museum collections and lab-reared colonies, including Natural History Museum, London [NHMUK], Texas Memorial Museum [TMM], South Australian Museum [SAM], Zoologisches Museum Berlin [ZMB], Muséum National d'Histoire Naturelle [MNHN], University Museum of Zoology in Cambridge [UMZC], University Museum of University of Tokyo [UMUT], and the Duke Lemur Centre [DLC]. Full specimen details including museum location and colony information (license numbers) can be found in Table S1.

All specimens were imaged using X-ray micro-Computed Tomography, with various instruments (Table S1 and S2): X-Tek HMX ST 225 (Nikon Metrology, Belgium), XT H 225 ST (Nikon Metrology, Belgium), Xradia MicroXCT-400 (Zeiss, USA), Inveon PET-CT (Siemens, USA), Skyscan 1072 (Bruker, USA), custom make CT scanner Helmholtz-Zentrum Berlin, SkyScan 1172 (Bruker, USA), μCT 50 (Scanco Medical AG, Switzerland), and ZEISS Xradia Versa 520 (Carl Zeiss X-ray Mircoscopy Inc., USA). Three-dimensional models of specimens were reconstructed using the specimen-specific voxel size (Table S1) in Avizo v.9.3 (FEI, OR, USA), based on

isosurface segmentation, allowing the extraction of 3D surface mesh models exported as.ply files. Meshes were decimated in Meshlab version 2020.7[123] to 1,000,000 faces, to reduce the computational demand without compromising mesh resolution. The resulting simplified 3D meshes were cleaned and prepared for subsequent geometric morphometric analysis using Geomagic Wrap (3D Systems). Cleaning involved the filling of any artefactual holes, the removal of vertebrae leaving only the skull elements within the 3D model. As the geometric morphometric analysis was performed on the left-hand side of the skull only, specimens that had an incomplete or damaged left-hand side of the skull (n=23) were mirrored[124] along the midline using the 'mirror' tool in Geomagic Wrap (3D Systems).

METHOD DETAILS

Characterisation of ontogeny

Centroid size (CS) is commonly used as a proxy for developmental age[43,125] when details regarding developmental age are unavailable. The species in this dataset span a large centroid size range from *Mus musculus* (adult CS = 87.58) to *Phacochoerus africanus* (adult CS = 1465.47). Thus, when all specimens are plotted together using CS (or logged CS) the small adult specimens of *Mus musculus* plot alongside fetal or infant specimens of larger species. Therefore, logged CS does not reflect these small adult specimens as adults (Figures S2A and S2B). To correct for differences in overall body size, we normalised CS for each species to their respective adult size (percentage of adult CS) (Equation 1). This percentage of adult CS was used as a continuous proxy for developmental age of each specimen (relative adult size) (Table S1).

$$Percentage\ of\ adult\ (\%) = \frac{CS\ of\ specimen\ x}{CS\ of\ adult\ of\ species\ x} \times 100 \quad \text{(Equation 1)}$$

In addition to this continuous proxy of age (relative adult size), we further assigned specimens discrete age categories using two approaches. Subsequently, we compared the two approaches and implemented in downstream analyses the approach that more accurately captured age. The first approach was based on specimen information from museum collection specimens, divided into fetal (F), infant (I), and adult (A) categories. The infant age category encompassed a particularly wide range of specimens and therefore was divided into two categories: infant and juvenile. Juvenile (J) was defined as the second eldest specimen for each species, as determined using the percentage of adult CS, described above. Where species had only one infant specimen, no juvenile was assigned to this species. However, species with multiple specimens that had a continuous age of >95% (based on the percentage of adult CS calculation) were all considered as juvenile. The 'fetal' stage for marsupials was assigned to any specimen with a known age <20 days old, and marsupial specimens with a similar level of ossification (following visual inspection) to those <20 days old, where absolute age data was unavailable. Qualitative visual assessment of ossification level indicated that these marsupial specimens reflected similar levels of ossification to fetal placental specimens. Of the specimens collected for the only monotreme in the dataset (*Ornithorhynchus anatinus*), the earliest stage that reflected the 'fetal' stage was excluded from the dataset due to the absence of >25% of the cranial bones. The next youngest specimen presented with a much higher level of maturity due to the highly ossified cranial bones and thus did not reflect a 'fetal' stage. Therefore, as no 'fetal' stage could be ascribed to the monotreme, this species was consequently excluded from any analyses that required an equal number of stages across species. The second discrete approach utilised the percentage of adult scores to subdivide specimens into four discrete categories at 25% intervals (Groups 1-4), with the hypothesis that these discrete age categories would be comparable to the fetal, infant, juvenile, and adult categories defined in the first approach. The two approaches were compared by plotting each specimen alongside the two developmental categories on a 3D principal components analysis (PCA), with shape on the x and y axes and age on the z-axis (Figure S2C). The 3D PCA showed little connection between the two approaches, with multiple fetal stages from the second approach appearing in the juvenile category of the first approach. Subsequently, we only implement the first discrete approach, that defined age category predominantly using visual inspection of specimens, for later analyses as this approach more accurately represented the developmental stage of each specimen. Across the dataset a total of 28 fetal specimens, 95 infant specimens, 20 juvenile specimens, and 22 adult specimens were identified.

Phylogeny

The most recent and extensive published mammalian phylogeny based on molecular data, dated with extensive fossil calibrations,[72] was used here for phylogenetically informed analyses. Nevertheless, phylogenetic correction was not used for all analyses due to the presence of multiple ontogenetic stages for the same species, which could not be compiled into a single phylogeny.[43] The time-calibrated maximum clade credibility phylogeny, that included 5,911 extant taxa, was trimmed to the 22 species in this dataset (Figure 1) using the '*keep.tip*' function in the *ape* R package.[126] Moreover, we cross-checked the marsupial topology of our trimmed phylogeny with that of the most recently published marsupial phylogeny.[127]

Developmental strategy

Mammals display a considerable range of developmental strategies, from highly altricial marsupials to precocial ungulates.[9] The altricial-precocial spectrum was defined here based on previous descriptions and definitions of the altricial-precocial spectrum within mammalian literature (Figure S4; Table S3), each species was assigned to one of the five categories (highly altricial, altricial, semi-altricial, semi-precocial, precocial).[9,10,58] Here, the highly altricial state is defined as resembling early fetal stages at birth. The altricial

state encompassed species with eyes and ears closed and with no hair when born. The semi-altricial state was used for species that retained closed eyes but had developed hair at birth. The semi-precocial state was defined as species with open sensory organs and had a greater parental reliance than precocial species. Finally, the precocial state encompassed species that were able to walk or run and feed on solid food shortly after birth. Species descriptions from the published literature were then used to determine the developmental strategy for each of the 22 species within the dataset, based on the described altricial-precocial spectrum (Table S3). Herein, the term developmental strategy is used to describe the position along the altricial-precocial spectrum for a species at birth.

Morphometric data collection

A total of 69 Type I (homology by biological definitions) and Type II (homology by geometric definitions) landmarks[128,129] were positioned, by a single assessor, on the left-hand side of the skull using the 'single point' tool in Stratovan Checkpoint (Stratovan Corporation, CA, USA) in order to capture cranial morphology (Figures 1B–1E; Table S4). Positioning of landmarks was complicated by the presence of fetal specimens within the dataset, as fetal specimens presented with incomplete bones and patchy ossification. In particular, the supraoccipital bone forms from two bilateral ossification centres,[130] resulting in early developmental specimens having a pair of bilateral supraoccipital bones that are not yet fused at the midline. In such cases (*Phataginus tricuspis*), landmarks 42 and 43 were positioned at the point of the supraoccipital that was closest to the midline.

Of these 69 landmarks, three were used as midline landmarks to mirror the manually positioned left-hand side landmarks onto the right-hand side of the skull (Table S1) and thus increase the specimen sample size. The presence of early developmental specimens, with paired bones not adjoining at the midline, meant that a common set of midline landmarks could not be implemented across the dataset. Instead, specimen-specific midline landmarks were selected to ensure the appropriate mirroring of landmarks and obtain a bilaterally symmetrical skull dataset. Mirrored landmarks were checked for accuracy on the meshes of all specimens using '*spheres3d*' in the *rgl* R package.[131]

A complete set of landmarks is required for every specimen within the dataset to perform geometric morphometric analyses.[132] Data collection avoided using incomplete specimens where possible; however, some instances of missing morphometric data were unavoidable to procure minimum sample sizes. Missing morphometric data was dealt with in one of two ways, depending on the type of missing data. Firstly, for damaged, broken, or missing bones due to artefacts of preservation, landmarks were positioned close to the missing region but 'toggled as missing' producing a landmark with an x, y, and z-coordinate value of 9999. The proportion of missing landmarks across the dataset was small, equating to less than 1% of the overall data. The missing landmarks were estimated using the '*estimate.missing*' function and thin-plate spline (TPS) method in the *geomorph* R package,[132] prior to mirroring and performing Procrustes superimposition on the landmarks. The TPS approach uses a reference specimen with a complete landmark dataset against which specimens are aligned to using the common set of landmarks where the 'space' between the homologous landmarks is calculated and used to interpolate the missing landmarks for the target specimen.[61] Whilst interpolation may introduce error, the vast majority of missing landmarks were closely surrounded by other placed landmarks, reducing the magnitude of error that may be introduced from interpolation. Moreover, following interpolation, landmarks were mirrored and visually inspected on specimen meshes to confirm appropriate positioning. Secondly, variably present bones (jugal, premaxilla, ventral premaxilla, interparietal, paraoccipital, and basisphenoid) (Table S1), that were either biologically absent in the species, developmentally absent (had not yet developed in young specimens), or were seamlessly fused with adjacent cranial bones were still represented by their homologous landmarks associated with the absent bone defined in Table S4. This approach followed, the protocol outlined by Bardua et al.[124] and ensured homology of landmark placement across the dataset. The most prominent variably present bone across the dataset was the interparietal which was either genuinely absent through ontogeny, for example in *Sminthopsis macroura*,[127] or commonly fused with the supraoccipital, for example in *Monodelphis domestica* and *Cyclopes didactylus*.[133] When these variably present bones were either genuinely absent or fused with no visible suture to the adjacent bone, the bone was represented by all associated landmarks being placed onto a fixed position, creating a "zero area" for the absent or seamlessly fused bone. The fixed position where landmarks were placed was determined as the point that best reflected the location of the absent region, usually the region from which the absent bone developed. For example, all landmarks for the interparietal were positioned at the anterior point of the supraoccipital as these bones were commonly fused and ossification of the interparietal typically begins at the dorsal anterior supraoccipital.[133] Absent variably present regions were therefore represented by a single coordinate, reflecting their lack of bony area. Following Procrustes superimposition, the absent variably present landmarks were corrected to ensure the absent variably present region was still reflected by a single coordinate position.

QUANTIFICATION AND STATISTICAL ANALYSIS

All analyses were performed in R v.3.6.1.[134]

Generalised Procrustes Analysis

Generalised Procrustes analysis (GPA)[135] was performed on all morphometric data to align the specimens by removing non-shape components (rotation, translation, and size).[136] GPA was performed on the mirrored landmark dataset using the '*gpagen*' function in the *geomorph* R package,[132] as a bilaterally symmetrical skull dataset produces a more accurate alignment of the specimens.[137,138] The mirrored right-side landmarks were removed following Procrustes superimposition, to reduce the dimensionality of the geometric morphometric dataset. All downstream analyses were therefore conducted on the left and midline only coordinate dataset.

Please cite this article in press as: White et al., Pedomorphosis in the ancestry of marsupial mammals, Current Biology (2023), https://doi.org/10.1016/j.cub.2023.04.009

Cranial morphology

We performed principal components analyses (PCA) on the Procrustes superimposed coordinate data, using the '*gm.prcomp*' function in the *geomorph* R package,[132] to assess the morphological variation across both the adult-only (n=22) and full developmental datasets (n=165). Extreme shapes were plotted along each principal component (PC) to visualise morphological variation. Firstly, a phylogenetic principal components analysis was performed for the dataset. Cranial variation across the major clades (Marsupialia, Xenarthra, Afrotheria, Laurasiatheria, and Euarchontoglires), for the adult-only dataset (n=22), was quantified using allometry-corrected Procrustes variances, by implementing the '*morphol.disparity*' function in the *geomorph* R package.[132] A second PCA for the full developmental dataset (n=165) was then conducted. This PCA for the full dataset was plotted indicating discrete and continuous age to assess the role of ontogeny on the evolution of cranial morphology. Similarly, allometry-corrected Procrustes variances were calculated to quantify multivariate morphological variation across the discrete age categories (fetal, infant, juvenile, and adult). Finally, PCs 1 and 2 from the PCA for the full developmental dataset were plotted against continuous developmental time (% of adult centroid size) (on the z-axis), with discrete developmental age also displayed as symbols, to visualise the dynamics of shape variation through ontogeny (note that this univariate comparison was not used in any statistical analysis, all of which used the full multivariate shape analyses).

Influences on cranial shape

The influence of developmental strategy on allometry-corrected multivariate skull shape was assessed by implementing ordinary least squares (OLS) regression in both a MANOVA for the entire developmental dataset ('*procD.lm*' function in *geomorph*) and phylogenetic MANOVA for the adult dataset ('*procD.pgls*' function in *geomorph*).[132] In both cases this was a regression between the residuals of the allometry fit (Procrustes shape variables $\sim$ log(Centroid size)) (i.e., allometry corrected shape) and the developmental strategy categories.

Allometry and ontogenetic trajectories

To test whether allometry (size-related shape change) explained a significant degree of shape variation in this dataset, a multivariate Procrustes regression was performed using the '*procD.lm*' function in the geomorph R package,[132] regressing Procrustes superimposed coordinates against their log-transformed centroid size (Procrustes shape variables $\sim$ log(centroid size)). Multivariate allometry was then compared pairwise across species (two species Procrustes shape variables $\sim$ two species log(centroid size)) and subject to Bonferroni correction to account for simultaneous multiple comparisons and reduce the risk of type 1 error.

In order to visualise shape change through ontogeny for specific components of cranial shape, ontogenetic trajectories were computed for each PC separately, following the protocol outlined in Morris et al.[32] Regressions were performed for each species between PC scores and log-transformed centroid size using the '*procD.lm*' function in the *geomorph* R package (PC axis scores $\sim$ log(centroid size)).[132] These univariate ontogenetic trajectories were then plotted for PC1 and PC2, although slope and intercept values were calculated for all 164 PCs (Table S7). As noted above, statistical comparisons were not performed on these univariate trajectories, due to the issues associated with univariate analysis.[75]

Ancestral estimation: Skull shape development

Using the phylogenetic framework described above, we estimated ancestral allometries, using species' multivariate allometries, for each major placental superorder (Xenarthra, Afrotheria, Laurasiatheria, and Euarchontoglires) and for the ancestral therian, marsupial, placental, and common ancestor of placentals, marsupials, and the monotreme (crown Mammalia) (Figure S3). This approach used species' multivariate Procrustes regression between multivariate shape and size (allometry formula: Procrustes shape variables $\sim$ log(centroid size)) to estimate ancestral slope and intercept coefficients under an assumption of Brownian evolution using maximum-likelihood by implementing the '*anc.ML*' function in the *phytools* R package,[139] as implemented by Morris et al.[32] Ancestral state estimation was also performed using an Ornstein-Uhlenbeck (OU) model of evolution by implementing the '*anc.ML*' function, although ancestral estimations were identical with this OU model to the Brownian model of evolution. Shape was plotted against log transformed centroid size, using the estimated slope and intercept coefficients, to visualise differences between reconstructed and species-specific allometries. Differences in slope and intercept were used to determine heterochronic shifts, as performed in Morris et al.[32] and Lanzetti et al.[140] Acceleration (peramorphosis) and deceleration (paedomorphosis) were identified from differences in slope, with acceleration indicated by a steeper slope (i.e., a faster rate of growth) and deceleration indicated by a shallower slope compared (i.e., a slower rate of growth) to the respective ancestral slope,[27,30] as illustration in Figure 1. Pre-displacement (peramorphosis) occurs when the onset of growth begins earlier in the descendent than the ancestral node, identifiable from a higher y-intercept,[27,30] as illustrated in Figure 1. In contrast, post-displacement (paedomorphosis) occurs when the onset of growth is delayed in the descendant compared with the ancestral node, identifiable from a lower y-intercept,[27,30] as illustrated in Figure 1.[27,30,32,43]